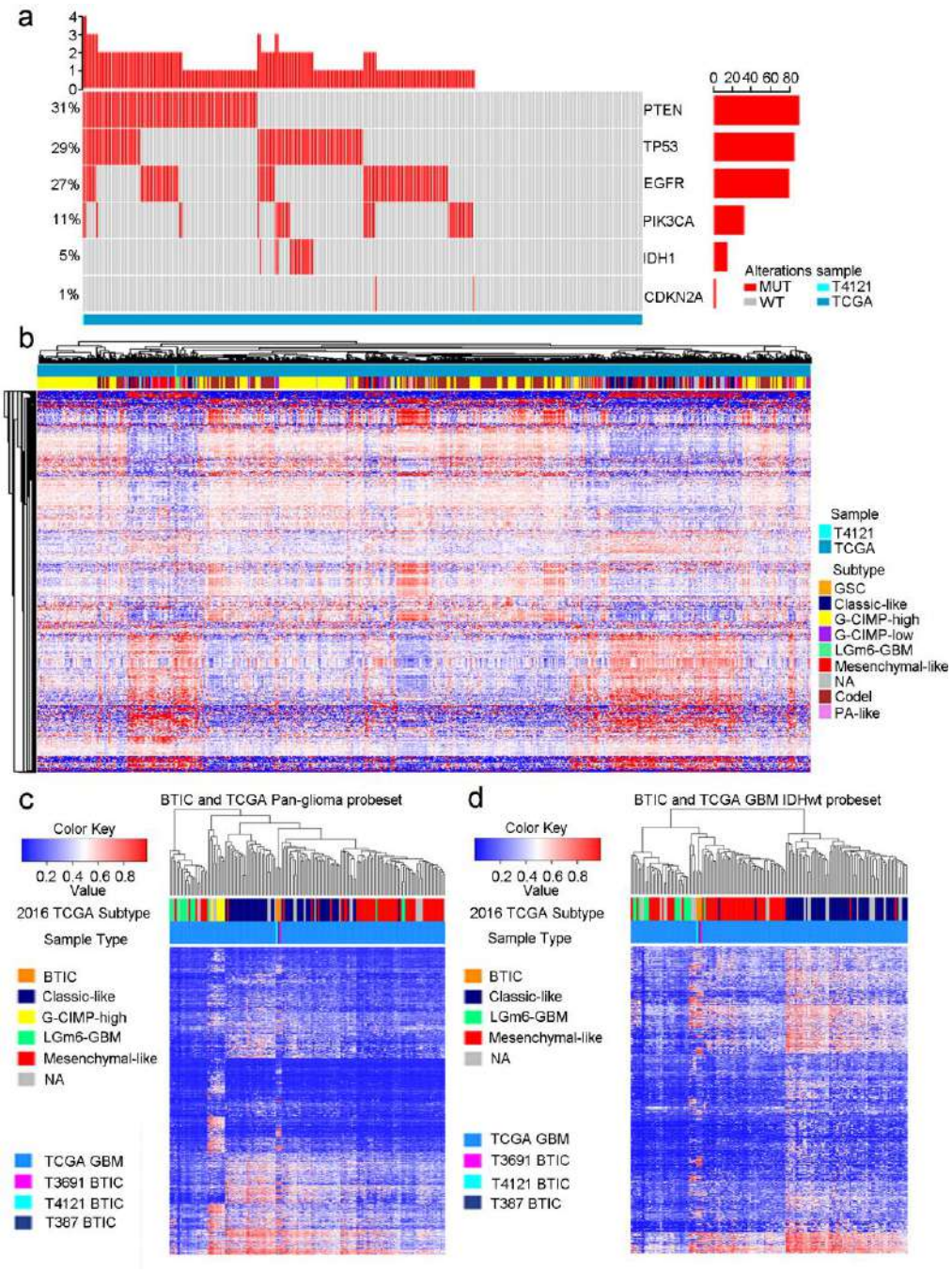

Supplementary Figure 1

Genomic profiles and epigenetic characterizations comparing TCGA glioma specimens and T4121 BTICs.

(**a**) Mutations in coding sequences of frequently mutated genes in glioblastoma were identified through whole exome sequencing. Top left legend: Number of genes mutated in the selected gene set per specimen. Right legend: Percentage of specimens harboring a mutation in each gene. (**b**) Following quantile normalization across samples and median centering of gene expression, the top 10% most variant genes were used to cluster low grade and high grade glioma samples with RNA-seq data from T4121 BTICs. (**c**) Hierarchical clustering on the Pan-glioma probe set (1,300 probes) of DNA methylation 450K array data from BTICs (n = 3) and TCGA GBM (n = 155). (**d**) Hierarchical clustering on the *IDH* wild type probe set (914 probes) from DNA methylation 450K array data from *IDH* wild type samples among TCGA GBM specimens (n = 149) and BTICs (n = 3).

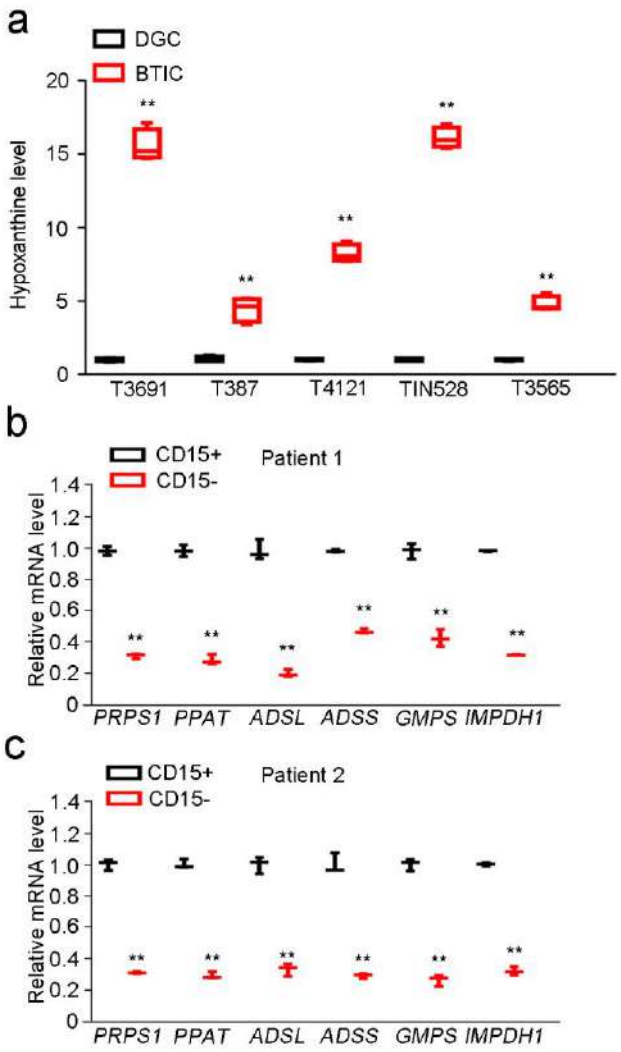

Supplementary Figure 2

BTICs contain elevated levels of purine degradation products compared to differentiated progeny.

Targeted mass spectrometry was performed to examine the level of a purine degradation product (hypoxanthine) using cell lysates of matched brain tumor initiating cells (BTICs) and differentiated glioma cells (DGCs) from five patient-derived glioblastoma specimens (T3691, T387, T4121, TIN528, and T3565). The relative levels of hypoxanthine were displayed normalized to DGCs. All statistical analyses were performed using two-tailed unpaired Student's t-test; **, $P < 0.01$; n = 4 independent experiments per group. (T3691, $P < 0.0001$, $t(6) = 26.710$; T387, $P = 0.0001$, $t(6) = 8.020$; T4121, $P < 0.0001$, $t(6) = 15.232$; TIN528, $P < 0.0001$, $t(6) = 48.811$; T3565, $P < 0.0001$, $t(6) = 13.688$.) (**b**,**c**) Upregulation of purine synthesis pathway genes in CD15+ BTICs. Surgical specimens from two patients newly diagnosed with glioblastomas were immediately dissociated and prospectively sorted with beads conjugated with an anti-CD15 antibody in the absence of culture. The mRNA levels of six purine synthesis pathway enzymes (*PRPS1*, *PPAT*, *ADSL*, *ADSS*, *GMPS*, and *IMPDH1*) were measured using quantitative RT-PCR in matched CD15+ and CD15- populations derived from these two primary glioblastoma specimens. All statistical analyses were performed using two-tailed unpaired Student's t-test; **, $P < 0.01$; n = 3 independent experiments per group. Data were presented as median ± s.e.m. (Patient 1: *PRPS1*, $P < 0.0001$, $t(4) = 34.461$; *PPAT*, $P < 0.0001$, $t(4) = 24.505$; *ADSL*, $P < 0.0001$, $t(4) = 19.579$; *ADSS*, $P < 0.0001$, $t(4) = 50.404$; *GMPS*, $P < 0.0001$, $t(4) = 13.235$; *IMPDH1*, $P < 0.0001$, $t(4) = 227.357$. Patient 2: *PRPS1*, $P < 0.0001$, $t(4) = 34.882$; *PPAT*, $P < 0.0001$, $t(4) = 34.345$; *ADSL*, $P < 0.0001$, $t(4) = 17.519$; *ADSS*, $P < 0.0001$, $t(4) = 19.213$; *GMPS*, $P < 0.0001$, $t(4) = 24.373$; *IMPDH1*, $P < 0.0001$, $t(4) = 39.910$.)

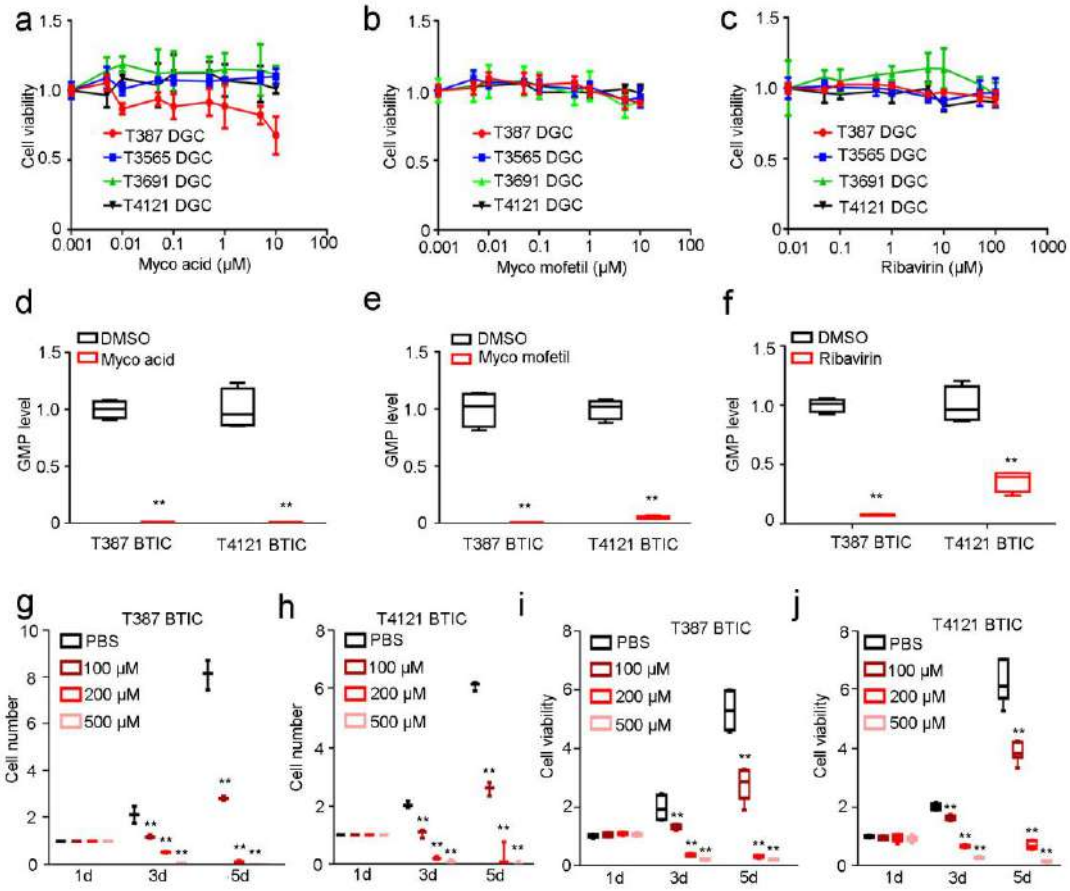

Supplementary Figure 3

Effects of purine synthesis inhibitors and AICAR.

(**a**-**c**) Sensitivity of four patient-derived DGC models (T387, T3565, T3691, and T4121) to three purine synthesis inhibitors: (**a**) mycophenolic acid, (**b**) mycophenolate mofetil, and (**c**) ribavirin. Data are presented as the mean ± s.e.m. (**d**-**f**) Purine synthesis inhibitors attenuate GMP synthesis in BTICs. Two patient-derived BTIC models (T387 and T4121) were treated with each agent at concentrations that induce cellular responses: (**d**) mycophenolic acid (5 μM), (**e**) mycophenolate mofetil (5 μM), or (**f**) ribavirin (50 μM). DMSO was used as vehicle control. GMP levels were determined using targeted mass spectrometry. All statistical analyses were performed using two-tailed unpaired Student's t-test; **, $P < 0.01$; n = 4 independent experiments per group. (Mycophenolic acid: T387, $P < 0.0001$, $t(6) = 26.220$; T4121, $P < 0.0001$, $t(6) = 11.383$. Mycophenolate mofetil: T387, $P < 0.0001$, $t(6) = 13.002$; T4121, $P < 0.0001$, $t(6) = 21.557$. Ribavirin: T387, $P < 0.0001$, $t(6) = 33.811$; T4121, p = 0.0002, $t(6) = 7.257$.) (**g**,**h**) Cell numbers of T387 and T4121 BTICs treated with 0, 100 μM, 200 μM, or 500 μM AICAR (5-aminoimidazole-4-carboxamide ribonucleotide). Time points were taken at days 1, 3, and 5. All statistical analyses were performed using two-tailed unpaired Student's t-test; *, $P < 0.05$; **, $P < 0.01$; n = 3 independent experiments per group. Data were presented as median ± s.e.m. (T387: day 3: 100 μM, $P = 0.0031$, $t(4) = 4.755$; 200 μM, $P = 0.0002$, $t(4) = 7.731$; 500 μM, $P < 0.0001$, $t(4) = 9.579$; day 5: 100 μM, $P < 0.0001$, $t(4) = 20.229$; 200 μM, $P < 0.0001$, $t(4) = 30.923$; 500 μM, $P < 0.0001$, $t(4) = 31.516$. T4121: day 3: 100 μM, $P < 0.0001$, $t(4) = 13.556$; 200 μM, $P < 0.0001$, $t(4) = 26.207$; 500 μM, $P < 0.0001$, $t(4) = 27.817$; day 5: 100 μM, $P < 0.0001$, $t(4) = 21.848$; 200 μM, $P < 0.0001$, $t(4) = 23.165$; 500 μM, $P < 0.0001$, $t(4) = 65.922$.) (**i**,**j**) Cell viability of T387 and T4121 BTICs treated with 0, 100 μM, 200 μM, or 500 μM AICAR (5-aminoimidazole-4-carboxamide ribonucleotide) was assessed by CellTiter-Glo. Time points were taken at days 1, 3, and 5. All statistical analyses were performed using two-tailed unpaired Student's t-test; *, $P < 0.05$; **, $P < 0.01$; n = 6 independent experiments per group. (T387: day 3: 100 μM, $P = 0.0022$, $t(10) = 4.089$; 200 μM, , $P < 0.0001$, $t(10) = 10.301$; 500 μM, $P < 0.0001$, $t(10) = 11.282$; day 5: 100 μM, $P < 0.0001$, $t(10) = 7.399$; 200 μM, $P < 0.0001$, $t(10) = 19.776$; 500 μM, $P < 0.0001$, $t(10) = 20.225$. T4121: day 3: 100 μM, $P < 0.0001$, $t(10) = 7.434$; 200 μM, $P < 0.0001$, $t(10) = 31.419$; 500 μM, $P < 0.0001$, $t(10) = 41.475$; day 5: 100 μM, $P < 0.0001$, $t(10) = 7.521$; 200 μM, $P < 0.0001$, $t(10) = 19.140$; 500 μM, $P < 0.0001$, $t(10) = 21.404$.)

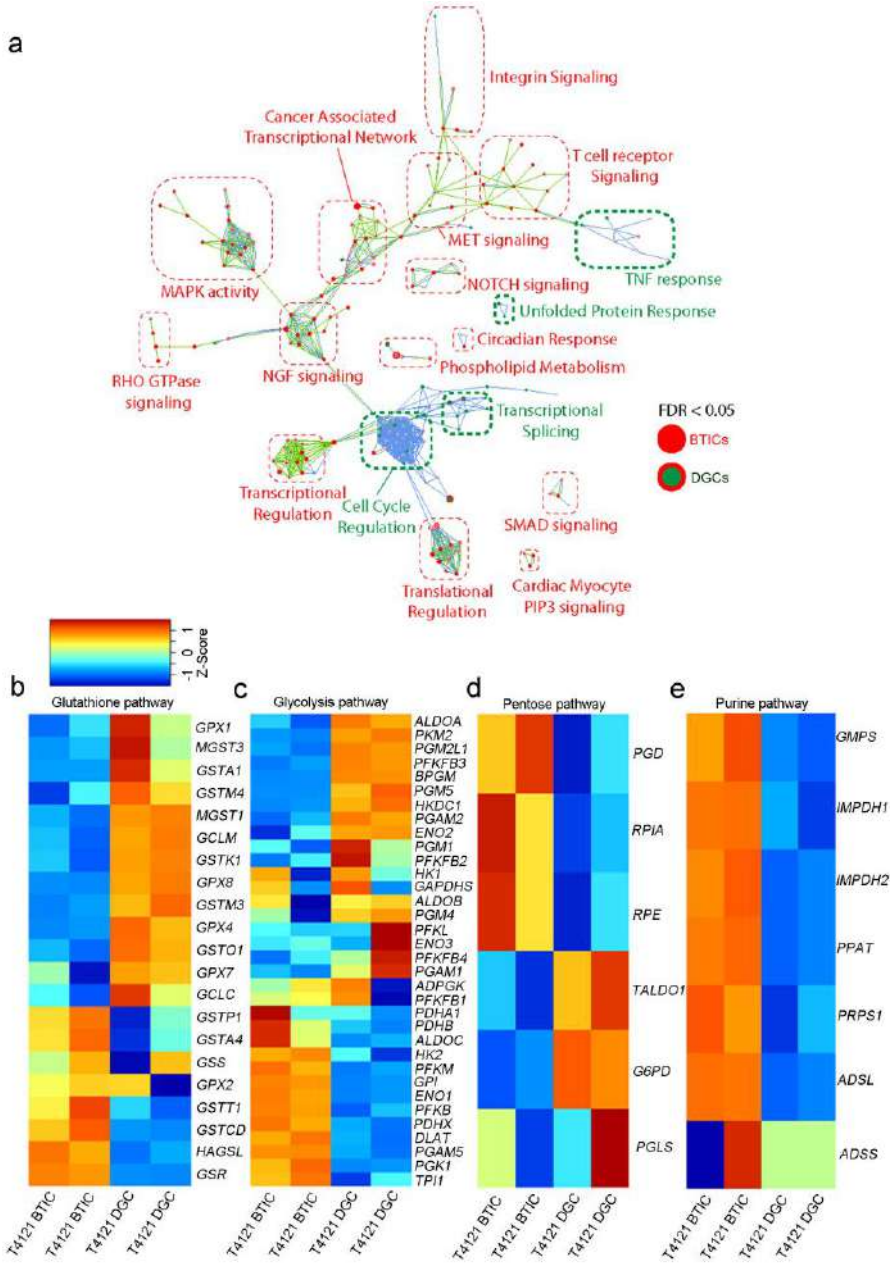

Supplementary Figure 4

Pathway analyses comparing BTICs to DGCs.

(**a**) Pathway map of enhancer associated gene network (identified with H3K27 acetylation ChIP-seq in T4121) comparing BTICs (red) versus DGCs (green). Pathways shown were identified using GREAT (http://bejerano.stanford.edu/great/public/html/), which was used to query the MSIGdb Broad pathway database (http://software.broadinstitute.org/gsea/msigdb/collections.jsp). Shown are networks with a FDR value of less than 0.05. (**b**-**e**) BTICs upregulate genes involved in the purine pathway. T4121 BTICs and DGCs underwent RNA-seq analysis in biologic duplicates with selective analysis of metabolic pathways, including (**b**) glutathione, (**c**) glycolysis, (**d**) pentose phosphate, and (**e**) purine biosynthesis. Z-scores were calculated from the $\log_2$ transformed FPKM values for each sample.

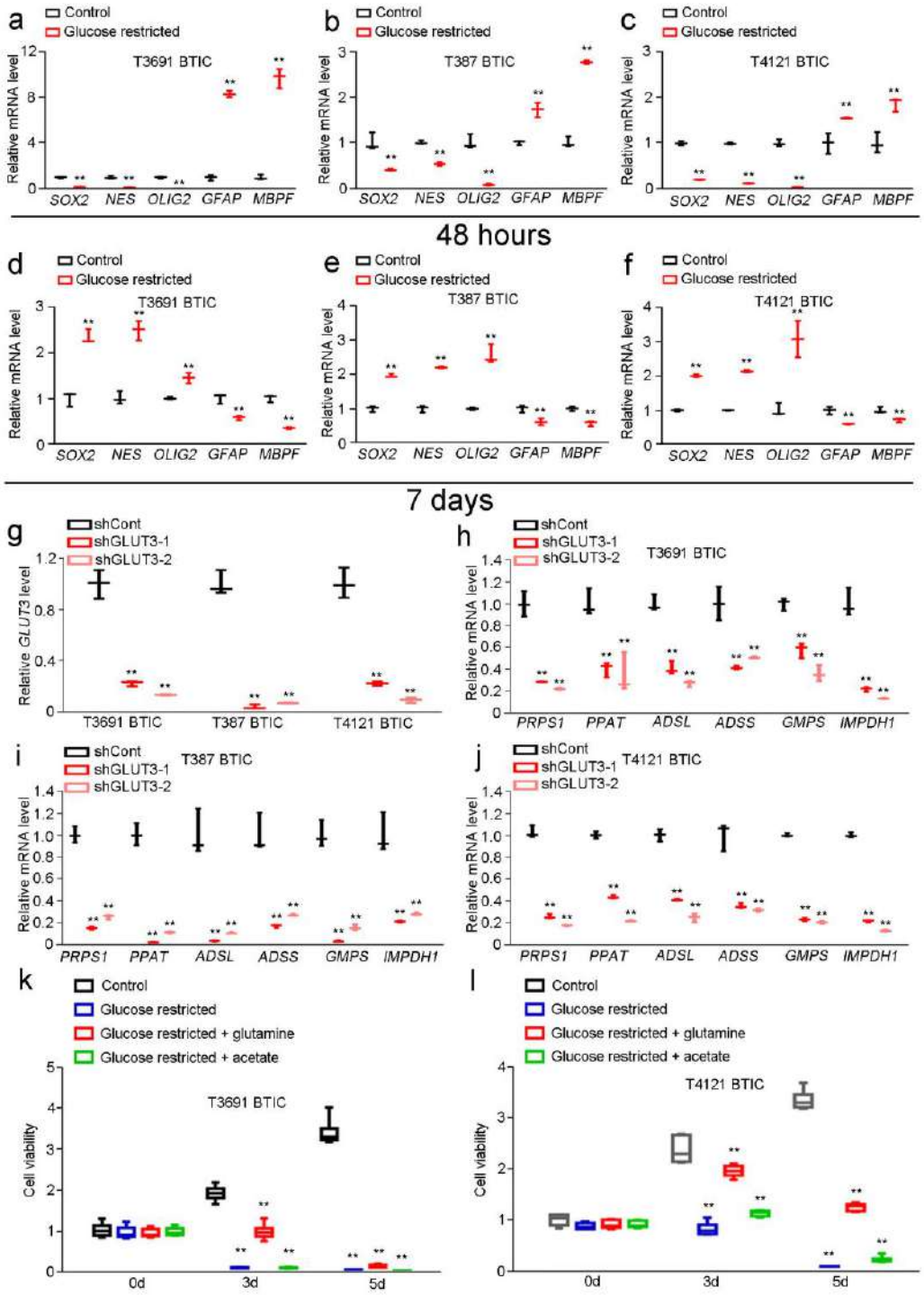

Supplementary Figure 5

Effects of short-term versus long-term glucose restriction and GLUT3 knockdown.

(**a**-**c**) Effect of glucose restricted conditions (0.45 g/L) and compared to standard conditions (4.5 g/L) for 48 hours on stemness markers in three BTIC models (**a**) T3691, (**b**) T387 and (**c**) T4121. Quantitative RT-PCR was then performed for stem cell markers, including *SOX2*, *NES*, and *OLIG2*, and differentiation markers, including *GFAP* and *MBPF*. All statistical analyses were

performed using two-tailed unpaired Student's t-test; **, $P < 0.01$; n = 3 independent experiments per group. Data were presented as median ± s.e.m. (T3691: *SOX2*, $P = 0.0002$, $t(4) = 11.262$; *NES*, $P < 0.0001$, $t(4) = 18.175$; *OLIG2*, $P < 0.0001$, $t(4) = 18.728$; *GFAP*, $P < 0.0001$, $t(4) = 34.228$; *MBPF*, $P < 0.0001$, $t(4) = 17.103$. T387: *SOX2*, $P < 0.0001$, $t(4) = 14.251$; *NES*, $P = 0.0029$, $t(4) = 5.385$; *OLIG2*, $P = 0.0003$, $t(4) = 9.799$; *GFAP*, $P = 0.0008$, $t(4) = 7.509$; *MBPF*, $P < 0.0001$, $t(4) = 25.319$. T4121: *SOX2*, $P < 0.0001$, $t(4) = 63.347$; *NES*, $P < 0.0001$, $t(4) = 30.664$; *OLIG2*, $P < 0.0001$, $t(4) = 22.384$; *GFAP*, $P = 0.0065$, $t(4) = 4.266$; *MBPF*, $P = 0.0026$, $t(4) = 5.513$.) (**d**-**f**) Effect of restricted glucose conditions (0.45 g/L) compared to standard conditions (4.5 g/L) for 7 days on stemness markers in three BTIC models (**d**) T3691, (**e**) T387, and (**f**) T4121. Quantitative RT-PCR was then performed for stem cell markers, including *SOX2*, *NES*, and *OLIG2*, and differentiation markers, including *GFAP* and *MBPF*. All statistical analyses were performed using two-tailed unpaired Student's t-test; **, $P < 0.01$; n = 3 independent experiments per group. (T3691: *SOX2*, $P = 0.0002$, $t(4) = 10.369$; *NES*, $P = 0.0003$, $t(4) = 10.074$; *OLIG2*, $P = 0.0015$, $t(4) = 6.409$; *GFAP*, $P = 0.0015$, $t(4) = 6.436$; *MBPF*, $P < 0.0001$, $t(4) = 14.048$. T387: *SOX2*, $P < 0.0001$, $t(4) = 16.883$; *NES*, $P < 0.0001$, $t(4) = 20.536$; *OLIG2*, $P = 0.0003$, $t(4) = 9.481$; *GFAP*, $P = 0.0047$, $t(4) = 4.699$; *MBPF*, $P = 0.0010$, $t(4) = 7.217$. T4121: *SOX2*, $P < 0.0001$, $t(4) = 35.185$; *NES*, $P < 0.0001$, $t(4) = 57.581$; *OLIG2*, $P = 0.0015$, $t(4) = 9.355$; *GFAP*, $P = 0.0017$, $t(4) = 6.183$; *MBPF*, $P = 0.0051$, $t(4) = 4.585$.) (**g**) Knockdown of *GLUT3* using two independent shRNAs decreased mRNA level of genes involved in purine synthesis in three BTIC models, T3691, T387 and T4121. All statistical analyses were performed using two-tailed unpaired Student's t-test; **, $P < 0.01$; n = 3 independent experiments per group. Data were presented as median ± s.e.m. (T3691: shGLUT3-1, $P = 0.0023$, $t(4) = 11.828$; shGLUT3-2, $P = 0.0017$, $t(4) = 13.453$; T387: shGLUT3-1, $P < 0.0001$, $t(4) = 17.209$; shGLUT3-2, $P < 0.0001$, $t(4) = 16.923$. T4121: shGLUT3-1, $P = 0.0007$, $t(4) = 13.700$; shGLUT3-2, $P = 0.0005$, $t(4) = 15.455$.) (**h**) Quantitative RT-PCR assessment of *PRPS1*, *PPAT*, *ADSL*, *ADSS*, *GMPS*, and *IMPDH1* mRNA levels in T3691 BTICs expressing shCont, shGLUT3-1, or shGLUT3-2. All statistical analyses were performed using two-tailed unpaired Student's t-test; **, $P < 0.01$; n = 3 independent experiments per group. Data were presented as median ± s.e.m. (T3691: *PRPS1*, shGLUT3-1, $P = 0.0036$, $t(4) = 10.693$; shGLUT3-2, $P = 0.0028$, $t(4) = 9.098$; *PPAT*, shGLUT3-1, $P = 0.0003$, $t(4) = 7.292$; shGLUT3-2, $P = 0.0041$, $t(4) = 5.102$; *ADSL*, shGLUT3-1, $P = 0.0029$, $t(4) = 8.948$; shGLUT3-2, $P = 0.0009$, $t(4) = 13.386$; *ADSS*, shGLUT3-1, $P = 0.0056$, $t(4) = 6.619$; shGLUT3-2, $P = 0.0100$, $t(4) = 7.136$; *GMPS*, shGLUT3-1, $P = 0.0021$, $t(4) = 8.058$. shGLUT3-2, $P = 0.0010$, $t(4) = 11.836$; *IMPDH1*, shGLUT3-1, $P = 0.0064$, $t(4) = 8.040$; shGLUT3-2, $P = 0.0047$, $t(4) = 8.966$.) (**i**) Quantitative RT-PCR assessment of *PRPS1*, *PPAT*, *ADSL*, *ADSS*, *GMPS*, and *IMPDH1* mRNA levels in T387 BTICs expressing shCont, shGLUT3-1, or shGLUT3-2. All statistical analyses were performed using two-tailed unpaired Student's t-test; **, $P < 0.01$; n = 3 independent experiments per group. Data were presented as median ± s.e.m. (T387: *PRPS1*, shGLUT3-1, $P < 0.0001$, $t(4) = 19.053$; shGLUT3-2, $P < 0.0001$, $t(4) = 16.493$; *PPAT*, shGLUT3-1, $P < 0.0001$, $t(4) = 16.840$; shGLUT3-2, $P = 0.0001$, $t(4) = 15.255$; *ADSL*, shGLUT3-1, $P = 0.0013$, $t(4) = 7.966$; shGLUT3-2, $P = 0.0018$, $t(4) = 7.371$; *ADSS*, shGLUT3-1, $P = 0.0012$, $t(4) = 8.168$, shGLUT3-2, $P = 0.0020$, $t(4) = 7.184$; *GMPS*, shGLUT3-1, $P = 0.0002$, $t(4) = 13.656$, shGLUT3-2, $P = 0.0003$, $t(4) = 11.689$; *IMPDH1*, shGLUT3-1, $P = 0.0017$, $t(4) = 7.527$; shGLUT3-2, $P = 0.0024$, $t(4) = 6.845$.) (**j**) Quantitative RT-PCR assessment of *PRPS1*, *PPAT*, *ADSL*, *ADSS*, *GMPS*, and *IMPDH1* mRNA levels in T4121 BTICs expressing shCont, shGLUT3-1, or shGLUT3-2. All statistical analyses were performed using two-tailed unpaired Student's t-test; **, $P < 0.01$; n = 3 independent experiments per group. Data were presented as median ± s.e.m. (T4121: *PRPS1*, shGLUT3-1, $P = 0.0003$, $t(4) = 18.993$; shGLUT3-2, $P = 0.0002$, $t(4) = 22.626$; *PPAT*, shGLUT3-1, $P = 0.0030$, $t(4) = 8.595$; shGLUT3-2, $P = 0.0015$, $t(4) = 8.029$; *ADSL*, shGLUT3-1, $P < 0.0001$, $t(4) = 18.242$; shGLUT3-2, $P < 0.0001$, $t(4) = 19.000$; *ADSS*, shGLUT3-1, $P = 0.0010$, $t(4) = 8.626$; shGLUT3-2, $P = 0.0007$, $t(4) = 9.225$; *GMPS*, shGLUT3-1, $P = 0.0015$, $t(4) = 10.968$; shGLUT3-2, $P = 0.0008$, $t(4) = 14.626$; *IMPDH1*, shGLUT3-1, $P < 0.0001$, $t(4) = 53.575$, shGLUT3-2, $P < 0.0001$, $t(4) = 61.720$.) (**k**,**l**) Glutamine partially rescued defects in cell proliferation induced by glucose restriction. Two BTIC models (**k**) T3691 and (**l**) T4121 were treated with restricted glucose conditions (0.45 g/L) compared to standard conditions (4.5 g/L). 2 mM glutamine or 100 μM acetate was used to rescue glucose restriction separately. Cell viability was measured by CellTiter-Glo. All statistical analyses were performed using two-tailed unpaired Student's t-test; **, $P < 0.01$; n = 6 independent experiments per group. (T3691 BTICs: Day 3, glucose restricted, $P < 0.0001$, $t(10) = 25.748$; glucose restricted + glutamine, $P < 0.0001$, $t(10) = 9.168$; glucose restricted + acetate, $P < 0.0001$, $t(10) = 25.762$; Day 5, glucose restricted, $P < 0.0001$, $t(10) = 26.061$; glucose restricted + glutamine, $P < 0.0001$, $t(10) = 25.288$; glucose restricted + acetate, $P < 0.0001$, $t(10) = 26.288$. T4121 BTICs: Day 3, glucose restricted, $P < 0.0001$, $t(10) = 13.688$; glucose restricted + glutamine, $P = 0.0043$, $t(10) = 3.676$; glucose restricted + acetate, $P < 0.0001$, $t(10) = 11.881$; Day 5, glucose restricted, $P < 0.0001$, $t(10) = 42.796$; glucose restricted + glutamine, $P < 0.0001$, $t(10) = 25.721$; glucose restricted + acetate, $P < 0.0001$, $t(10) = 39.037$.)

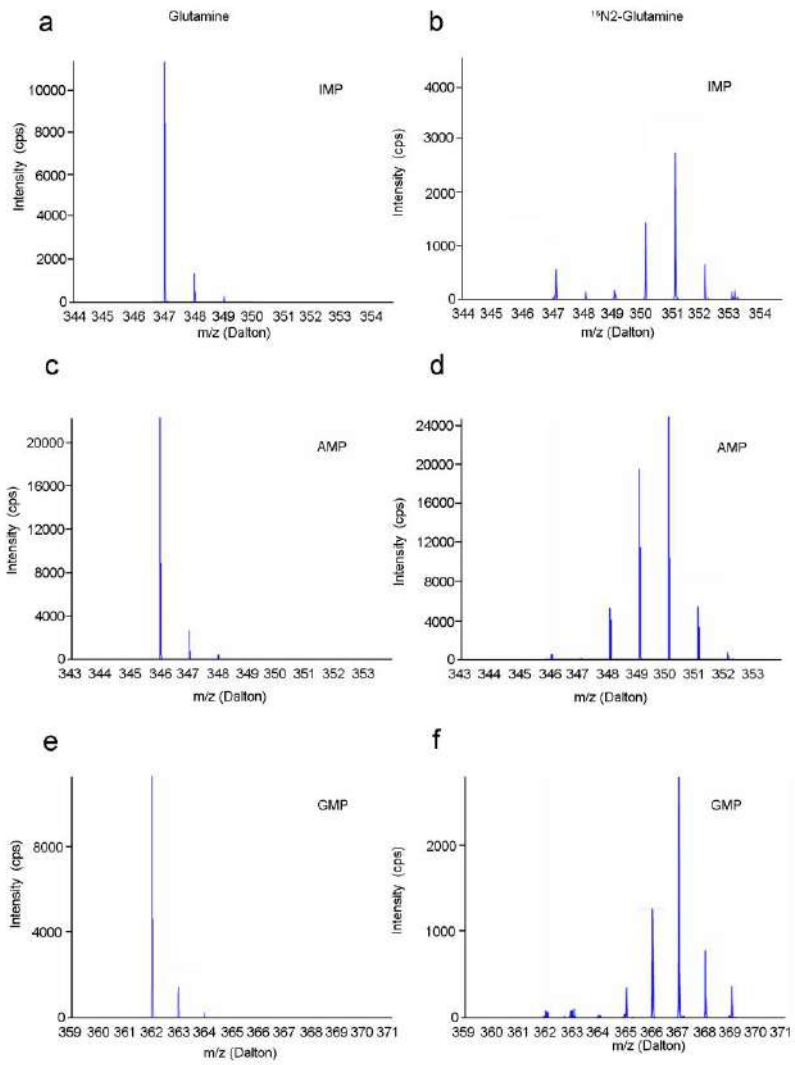

Supplementary Figure 6

Nitrogen tracing in BTICs using [$^{15}N_2$]glutamine.

(**a**-**f**) Targeted mass spectrometry was used to examine the levels of (**a**,**b**) IMP, (**c**,**d**) AMP, and (**e**,**f**) GMP using cell lysates of BTICs and matched DGCs from patient-derived glioblastoma specimen T387 treated with media containing either 2 mM regular glutamine or 2 mM ^{15}N2-glutamine, respectively, for 24 hours before harvesting.

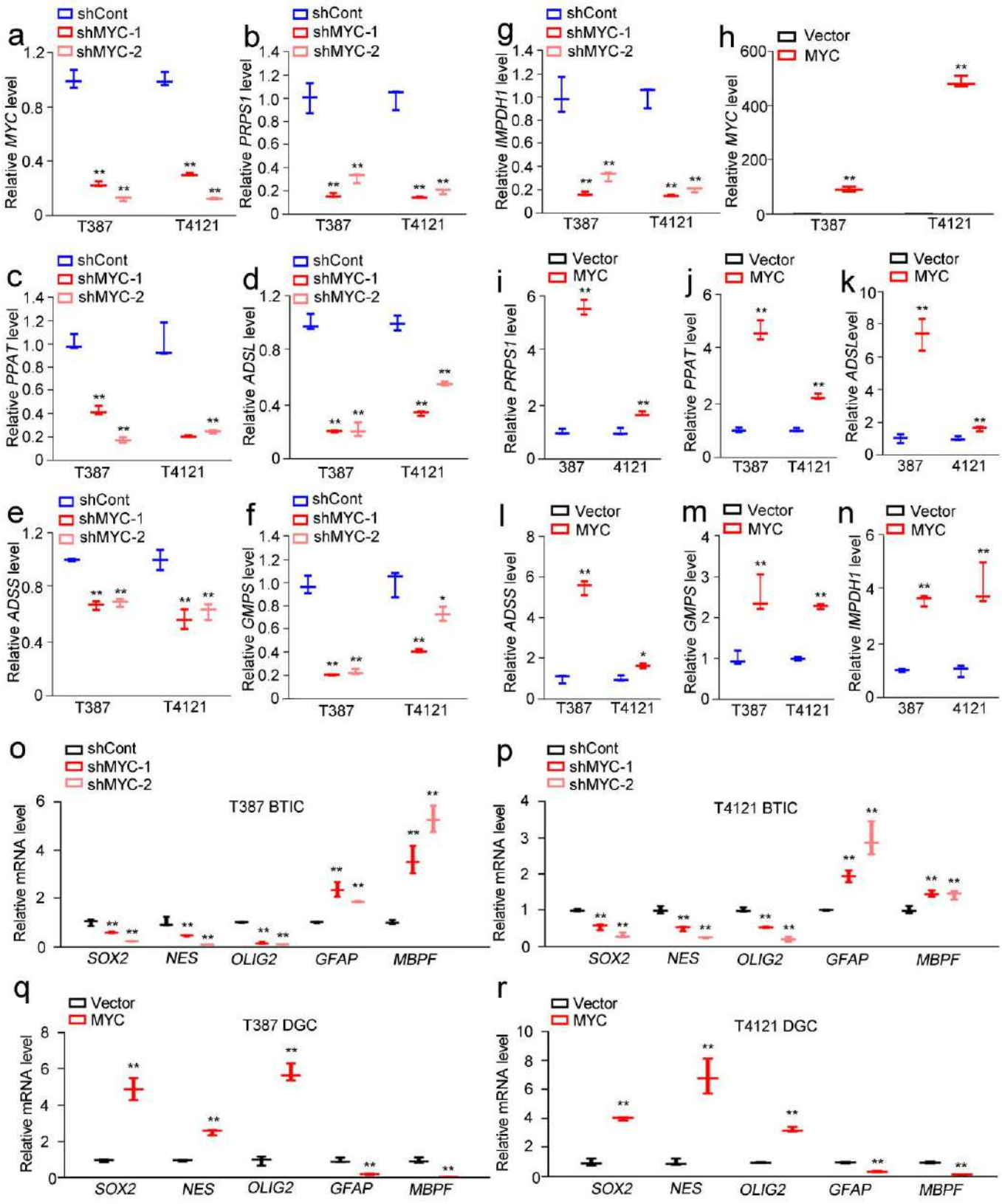

Supplementary Figure 7

Transcription factor MYC regulates mRNA levels of purine synthesis pathway genes in BTICs.

(**a**-**g**) Knockdown of *MYC* using two independent shRNAs decreased mRNA levels of genes involved in purine synthesis in BTICs. Quantitative RT-PCR assessment of *MYC*, *PRPS1*, *PPAT*, *ADSL*, *ADSS*, *GMPS*, and *IMPDH1* mRNA levels in T387 and T4121 BTICs expressing shCont, shMYC-1, or shMYC-2. All statistical analyses were performed using two-tailed unpaired Student's t-test; *, $P < 0.05$; **, $P < 0.01$; n = 3 independent experiments per group. Data were presented as median ± s.e.m. (**a**) *MYC* levels: T387: shMYC-1, $P = 0.0005$, $t(4) = 14.853$; shMYC-2, $P = 0.0003$, $t(4) = 17.277$. T4121: shMYC-1, $P = 0.0004$, $t(4) = 17.929$; shMYC-2, $P = 0.0002$, $t(4) = 22.822$. (**b**) *PRPS1* levels: T387: shMYC-1, $P < 0.0001$, $t(4) = 26.097$; shMYC-2, $P = 0.0002$, $t(4) = 11.178$. T4121: shMYC-1, $P = 0.0063$, $t(4) = 9.693$; shMYC-2, $P = 0.0021$, $t(4) = 7.116$. (**c**) *PPAT* levels: T387: shMYC-1, $P = 0.0002$, $t(4) = 13.522$; shMYC-2, $P < 0.0001$, $t(4) = 21.005$. T4121: shMYC-1, $P = 0.0011$, $t(4) = 9.169$; shMYC-2, $P = 0.0014$, $t(4) = 8.675$. (**d**) *ADSL* levels: T387: shMYC-1, $P < 0.0001$, $t(4) = 23.201$; shMYC-2, $P < 0.0001$, $t(4) = 17.491$. T4121: shMYC-1, $P < 0.0001$, $t(4) = 20.244$; shMYC-2, $P = 0.0002$, $t(4) = 13.751$. (**e**) *ADSS* levels: T387: shMYC-1, $P < 0.0001$, $t(4) = 17.853$; shMYC-2, $P < 0.0001$, $t(4) = 17.784$. T4121: shMYC-1, $P = 0.0002$, $t(4) = 7.265$; shMYC-2, $P = 0.0003$, $t(4) = 6.901$. (**f**) *GMPS* levels: T387: shMYC-1, $P < 0.0001$, $t(4) = 17.462$; shMYC-2, $P < 0.0001$, $t(4) = 16.212$. T4121: shMYC-1, $P = 0.0035$, $t(4) = 8.809$; shMYC-2, $P = 0.0234$, $t(4) = 3.256$. (**g**) *IMPDH1* levels: T387: shMYC-1, $P = 0.0005$, $t(4) = 11.061$; shMYC-2, $P = 0.0007$, $t(4) = 8.687$. T4121: shMYC-1, $P < 0.0001$, $t(4) = 50.570$; shMYC-2, $P < 0.0001$, $t(4) = 39.171$. (**h**-**n**) Overexpression of exogenous *MYC* upregulates mRNA levels of genes involved in purine synthesis pathway in BTICs. Quantitative RT-PCR assessment of *PRPS1*, *PPAT*, *ADSL*, *ADSS*, *GMPS*, and *IMPDH1* mRNA levels in T387 and T4121 BTICs expressing empty vector (Vector) or *MYC* overexpression vector (Myc). All statistical analyses were performed using two-tailed unpaired Student's t-test; *, $P < 0.05$; **, $P < 0.01$; n = 3 independent experiments per group. Data were presented as median ± s.e.m. (**h**) *MYC* levels: T387: p = 4.76e-05. , $t(4) = 18.750$. T4121: p = 1.85e-06. $t(4) = 42.371$. (**i**) *PRPS1* levels: T387: $P = 0.0072$, $t(4) = 16.118$. T4121: $P = 0.0054$, $t(4) = 7.577$. (**j**) *PPAT* levels: T387: $P < 0.0001$, $t(4) = 17.038$. T4121: $P < 0.0001$, $t(4) = 17.734$. (**k**) *ADSL* levels: T387: $P = 0.0010$, $t(4) = 10.814$. T4121: $P = 0.0082$, $t(4) = 5.112$. (**l**) *ADSS* levels: T387: $P < 0.0001$, $t(4) = 19.064$. T4121: $P = 0.0120$, $t(4) = 4.923$. (**m**) *GMPS* levels: T387: $P = 0.0054$, $t(4) = 5.487$. T4121: $P < 0.0001$, $t(4) = 31.383$. (**n**) *IMPDH1* levels: T387: $P = 0.0004$, $t(4) = 14.926$. T4121: $P = 0.0027$, $t(4) = 6.588$. (**o**,**p**) MYC regulates stemness markers in BTICs. Expression of *MYC* was knocked down using two non-overlapping shRNAs in (**o**) T387 and (**p**) T4121 BTICs. Quantitative RT-PCR was performed for precursor markers, including *SOX2*, *NES*, and *OLIG2*, and differentiation markers, including *GFAP* and *MBPF*. All statistical analyses were performed using two-tailed unpaired Student's t-test; **, $P < 0.01$; n = 3 independent experiments per group. Data were presented as median ± s.e.m. (**o**) T387: *SOX2*, shRNA1, $P = 0.0035$, $t(4) = 5.077$; shRNA2, $P = 0.0003$, $t(4) = 9.675$. *NES*, shRNA1, $P = 0.0044$, $t(4) = 4.775$; shRNA2, $P = 0.0006$, $t(4) = 8.081$. *OLIG2*, shRNA1, $P < 0.0001$, $t(4) = 30.207$; shRNA2, $P < 0.0001$, $t(4) = 51.140$. *GFAP*, shRNA1, $P = 0.0008$, $t(4) = 7.698$; shRNA2, $P < 0.0001$, $t(4) = 30.218$. *MBPF*, shRNA1, $P = 0.0007$, $t(4) = 7.748$; shRNA2, $P < 0.0001$, $t(4) = 13.316$. (**p**) T4121: *SOX2*, shRNA1, $P = 0.0005$, $t(4) = 8.549$; shRNA2, $P < 0.0001$, $t(4) = 14.691$. *NES*, shRNA1, $P = 0.0010$, $t(4) = 7.237$; shRNA2, $P < 0.0001$, $t(4) = 13.479$. *OLIG2*, shRNA1, $P = 0.0001$, $t(4) = 12.169$; shRNA2, $P < 0.0001$, $t(4) = 15.191$. *GFAP*, shRNA1, $P = 0.0003$, $t(4) = 9.957$; shRNA2, $P = 0.0010$, $t(4) = 7.318$. *MBPF*, shRNA1, $P = 0.0021$, $t(4) = 5.865$; shRNA2, $P = 0.0044$, $t(4) = 4.786$. (**q**,**r**) MYC induces stemness markers in DGCs. *MYC* was transduced into in (**o**) T387 and (**p**) T4121 DGCs using a lentiviral construct. An empty lentiviral vector was used as a negative control. Quantitative RT-PCR was performed for precursor markers (*SOX2*, *NES*, and *OLIG2*), and differentiation markers (*GFAP* and *MBPF*). All statistical analyses were performed using two-tailed unpaired Student's t-test; **, $P < 0.01$; n = 3 independent experiments per group. Data were presented as median ± s.e.m. (**q**) T387: *SOX2*, $P = 0.0002$, $t(4) = 11.187$; *NES*, $P < 0.0001$, $t(4) = 15.998$; *OLIG2*, $P < 0.0001$, $t(4) = 15.315$; *GFAP*, $P = 0.0004$, $t(4) = 9.214$; *MBPF*, $P = 0.0002$, $t(4) = 10.481$. (**r**) T4121: *SOX2*, $P < 0.0001$, $t(4) = 19.782$; *NES*, $P = 0.0006$, $t(4) = 8.348$; *OLIG2*, $P < 0.0001$, $t(4) = 23.285$; *GFAP*, $P < 0.0001$, $t(4) = 14.848$; *MBPF*, $P < 0.0001$, $t(4) = 23.382$.

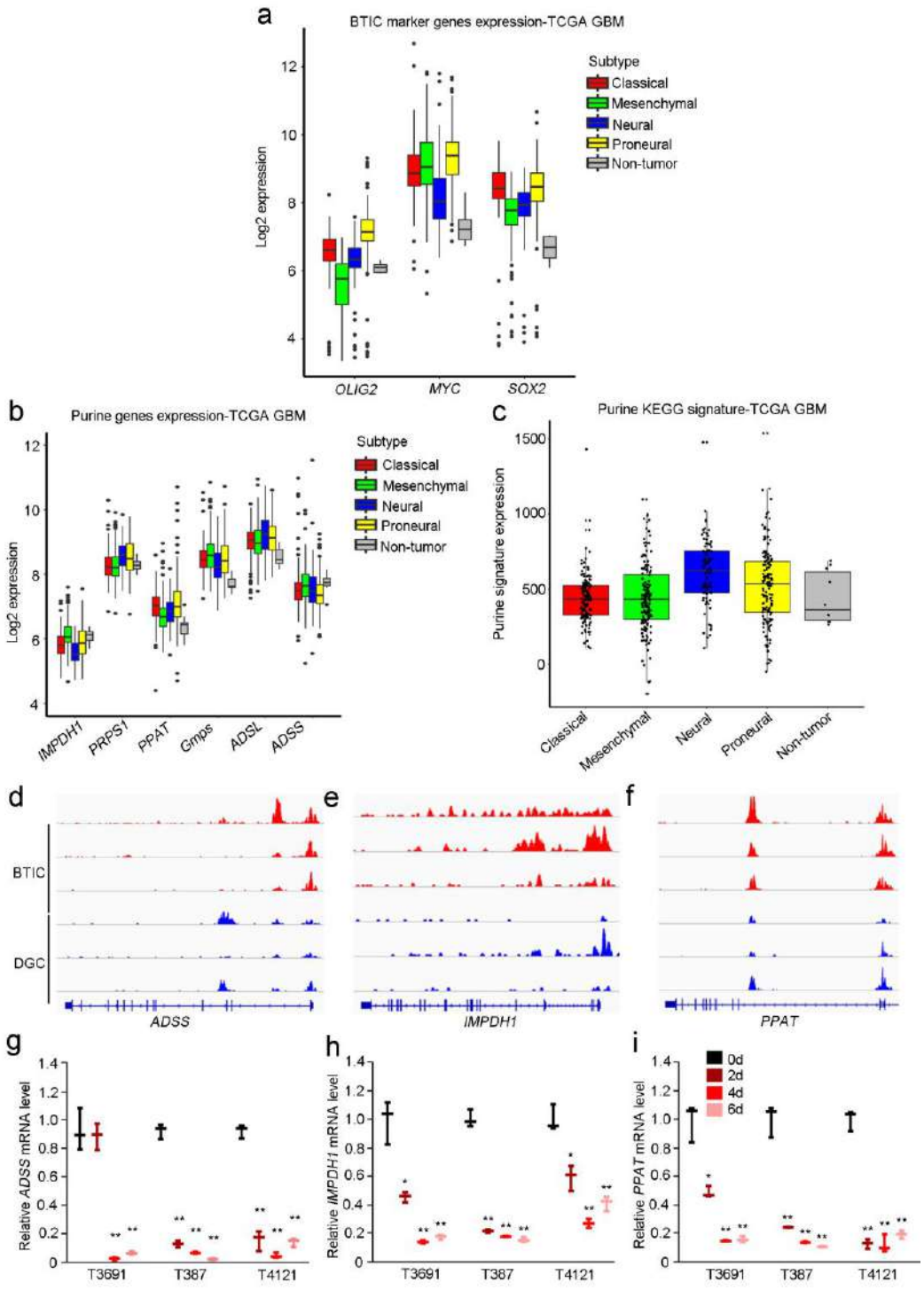

Supplementary Figure 8

Purine pathway gene expression analysis by subtype from TCGA datasets.

(**a**-**c**) The expression levels of (**a**) individual precursor marker mRNAs (*OLIG2*, *MYC*, and *SOX2*), (**b**) individual purine synthesis pathway mRNAs (*IMPDH1*, *PRPS1*, *PPAT*, *GMPS*, *ADSL*, and *ADSS*), and (**c**) purine pathway expression signature based on KEGG definition, from the TCGA dataset were plotted by four subtypes (Classical, Mesenchymal, Neural, and Proneural) as designated by the Verhaak 2010 paradigm. (**d**-**f**) *PPAT*, *ADSS*, and *IMPDH1* are upregulated in BTICs. H3K27ac ChIP-seq

enrichment plots centered at the gene locus for (**d**) *ADSS*, (**e**) *IMPDH1*, and (**f**) *PPAT* were displayed. Enrichment is shown for three matched pairs of DGCs and BTICs from patient-derived glioblastoma specimens. H3K27ac ChIP-seq data were downloaded from NCBI Gene Expression Omnibus (GEO) GSE54047. (**g**-**i**) qRT-PCR quantification of *ADSS*, *IMPDH1*, or *PPAT* mRNA levels in three patient-derived BTIC models during differentiation. BTICs derived from three primary human glioblastoma specimens (T3691, T387, T4121) were treated with serum to induce differentiation, with time points taken at 2, 4, and 6 days. All statistical analyses were performed using two-tailed unpaired Student's t-test; *, $P < 0.05$; **, $P < 0.01$; n = 3 independent experiments per group. Data were presented as median ± s.e.m. (*ADSS*: T3691, 2d, $P = 0.7400$, $t(4) = 0.353$; 4d, $P = 0.0005$, $t(4) = 10.524$; 6d, $P = 0.0006$, $t(4) = 10.049$; T387, 2d, $P < 0.0001$, $t(4) = 24.171$; 4d, $P < 0.0001$, $t(4) = 28.101$; 6d, $P < 0.0001$, $t(4) = 29.636$; T4121, 2d, $P < 0.0001$, $t(4) = 15.710$; 4d, $P < 0.0001$, $t(4) = 15.975$; 6d, $P < 0.0001$, $t(4) = 24.548$. *IMPDH1*: T3691, 2d, $P = 0.0133$, $t(4) = 3.996$; 4d, $P = 0.0024$, $t(4) = 6.522$; 6d, $P = 0.0029$, $t(4) = 6.237$; T387, 2d, $P < 0.0001$, $t(4) = 19.792$; 4d, $P < 0.0001$, $t(4) = 22.904$; 6d, $P < 0.0001$, $t(4) = 22.964$; T4121, 2d, $P = 0.0105$, $t(4) = 4.553$; 4d, $P = 0.0049$, $t(4) = 8.337$; 6d, $P = 0.0017$, $t(4) = 6.913$. *PPAT*: T3691, 2d, $P = 0.0200$, $t(4) = 4.784$; 4d, $P = 0.0033$, $t(4) = 7.025$; 6d, $P = 0.0035$, $t(4) = 7.681$; T387, 2d, $P < 0.0001$, $t(4) = 21.370$; 4d, $P < 0.0001$, $t(4) = 24.175$; 6d, $P < 0.0001$, $t(4) = 25.004$; T4121, 2d, $P < 0.0001$, $t(4) = 18.839$; 4d, $P < 0.0001$, $t(4) = 15.865$; 6d, $P < 0.0001$, $t(4) = 18.083$.)

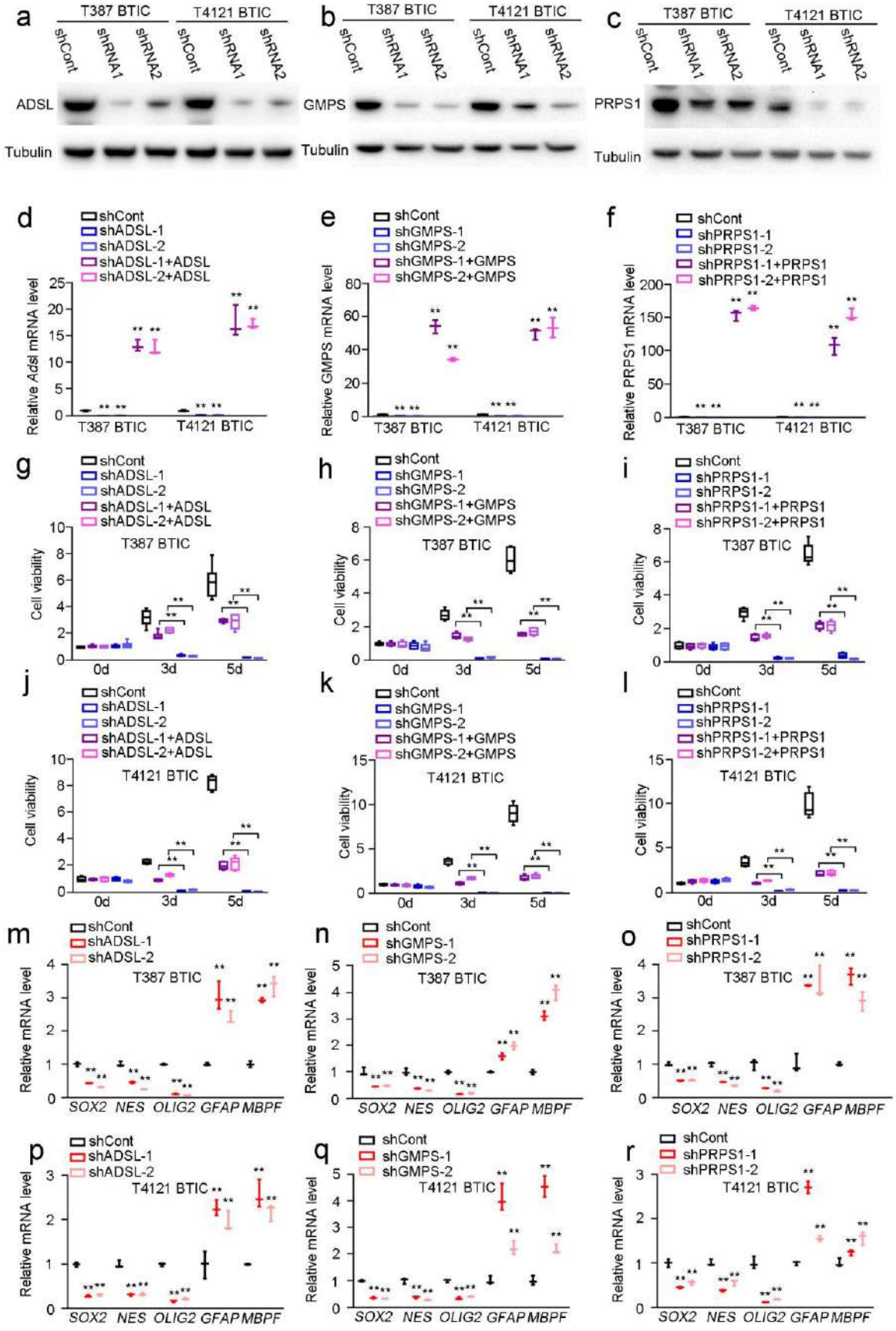

Nature Neuroscience: doi:10.1038/nn.4537

Supplementary Figure 9

Confirmation and reconstitution of ADSL, GMPS or *PRPS1* knockdown.

(**a**) Confirmation of *ADSL* knockdown effect in BTICs (T387 and T4121) (**b**) Confirmation of *GMPS* knockdown effect in BTICs (T387 and T4121). (**c**) Confirmation of *PRPS1* knockdown effect in BTICs (T387 and T4121). (**d**-**f**) Reconstitution of shRNA-mediated knockdown of purine synthesis genes in BTICs. Expression constructs for human ADSL, GMPS< and *PRPS1*, which were resistant to the respective shRNAs, were used to reconstitute the expression of corresponding genes in two BTIC models, T387 and T4121. All statistical analyses were performed using two-tailed unpaired Student's t-test; **, $P < 0.01$; n = 3 independent experiments per group. Data were presented as median ± s.e.m. (**d**) *ADSL*: T387, shADSL-1, $P < 0.0001$, $t(4) = 15.560$, shADSL-2, $P < 0.0001$, $t(4) = 14.701$; shADSL-1 + *ADSL*, $P < 0.0001$, $t(4) = 19.428$; shADSL-2 + *ADSL*, $P < 0.0001$, $t(4) = 13.765$; T4121, shADSL-1, $P = 0.0001$, $t(4) = 11.904$, shADSL-2, $P = 0.0003$, $t(4) = 11.571$; shADSL-1 + *ADSL*, $P = 0.0002$, $t(4) = 9.588$; shADSL-2 + *ADSL*, $P < 0.0001$, $t(4) = 29.885$. (**e**) *GMPS*: T387, shGMPS-1, $P = 0.0001$, $t(4) = 12.301$, shGMPS-2, $P = 0.0002$, $t(4) = 11.375$; shGMPS-1 + *GMPS*, $P < 0.0001$, $t(4) = 22.867$; shGMPS-2 + *GMPS*, $P < 0.0001$, $t(4) = 58.042$; T4121, shGMPS-1, $P < 0.0001$, $t(4) = 17.121$, shGMPS-2, $P < 0.0001$, $t(4) = 13.955$; shGMPS-1 + *GMPS*, $P < 0.0001$, $t(4) = 4.795$; shGMPS-2 + *GMPS*, $P < 0.0001$, $t(4) = 15.223$. (**f**) *PRPS1*: T387, shPRPS1-1, $P = 0.0003$, $t(4) = 10.059$, shPRPS1-2, $P = 0.0003$, $t(4) = 9.448$; shPRPS1-1 + *PRPS1*, $P < 0.0001$, $t(4) = 32.778$; shPRPS1-2 + *PRPS1*, $P < 0.0001$, $t(4) = 84.438$; T4121, shPRPS1-1, $P < 0.0001$, $t(4) = 20.042$, shPRPS1-2, $P < 0.0001$, $t(4) = 18.371$; shPRPS1-1 + *PRPS1*, $P < 0.0001$, $t(4) = 14.407$; shPRPS1-2 + *PRPS1*, $P < 0.0001$, $t(4) = 29.308$. (**g**-**i**) Cell viability was measured on T387 BTICs with reconstitution of (**g**) *ADSL*, (**h**) *GMPS*, or (**i**) *PRPS1* upon targeting each gene. BTICs expressing shCont were used as positive controls, and BTICs expressing shRNA targeting each gene without reconstitution were used as negative controls. All statistical analyses were performed using two-tailed unpaired Student's t-test; **, $P < 0.01$; n = 6 independent experiments per group. (**g**) *ADSL*: 3d, shCont vs. shADSL-1, $P < 0.0001$, $t(10) = 11.702$; shCont vs. shADSL-2, $P < 0.0001$, $t(10) = 12.057$; shADSL-1 vs. shADSL-1 + *ADSL*, $P < 0.0001$, $t(10) = 12.419$; shADSL-2 vs. shADSL-2 + *ADSL*, $P < 0.0001$, $t(10) = 23.708$; 5d, shCont vs. shADSL-1, $P < 0.0001$, $t(10) = 11.940$; shCont vs. shADSL-2, $P < 0.0001$, $t(10) = 12.030$; shADSL-1 vs. shADSL-1 + *ADSL*, $P < 0.0001$, $t(10) = 50.707$; shADSL-2 vs. shADSL-2 + *ADSL*, $P < 0.0001$, $t(10) = 12.524$. (**h**) *GMPS*: 3d, shCont vs. shGMPS-1, $P < 0.0001$, $t(10) = 21.323$; shCont vs. shGMPS-2, $P < 0.0001$, $t(10) = 20.689$; shGMPS-1 vs. shGMPS-1 + *GMPS*, $P < 0.0001$, $t(10) = 19.455$; shGMPS-2 vs. shGMPS-2 + *GMPS*, $P < 0.0001$, $t(10) = 27.714$; 5d, shCont vs. shGMPS-1, $P < 0.0001$, $t(10) = 21.273$; shCont vs. shGMPS-2, $P < 0.0001$, $t(10) = 21.327$; shGMPS-1 vs. shGMPS-1 + *GMPS*, $P < 0.0001$, $t(10) = 45.018$; shGMPS-2 vs. shGMPS-2 + *GMPS*, $P < 0.0001$, $t(10) = 18.834$. (**i**) *PRPS1*: 3d, shCont vs. shPRPS1-1, $P < 0.0001$, $t(10) = 21.930$; shCont vs. shPRPS1-2, $P < 0.0001$, $t(10) = 22.394$; shPRPS1-1 vs. shPRPS1-1 + *PRPS1*, $P < 0.0001$, $t(10) = 16.273$; shPRPS1-2 vs. shPRPS1-2 + *PRPS1*, $P < 0.0001$, $t(10) = 27.214$; 5d, shCont vs. shPRPS1-1, $P < 0.0001$, $t(10) = 24.397$; shCont vs. shPRPS1-2, $P < 0.0001$, $t(10) = 25.813$; shPRPS1-1 vs. shPRPS1-1 + *PRPS1*, $P < 0.0001$, $t(10) = 17.896$; shPRPS1-2 vs. shPRPS1-2 + *PRPS1*, $P < 0.0001$, $t(10) = 16.070$. (**j**-**l**) Cell viability was measured on T4121 BTICs with reconstitution of (**j**) *ADSL*, (**k**) *GMPS*, or (**l**) *PRPS1* upon targeting each gene. BTICs expressing shCont were used as positive controls, and BTICs expressing shRNA targeting each gene without reconstitution were used as negative controls. All statistical analyses were performed using two-tailed unpaired Student's t-test; **, $P < 0.01$; n = 6 independent experiments per group. (**j**) *ADSL*: 3d, shCont vs. shADSL-1, $P < 0.0001$, $t(10) = 21.756$; shCont vs. shADSL-2, $P < 0.0001$, $t(10) = 20.821$; shADSL-1 vs. shADSL-1 + *ADSL*, $P < 0.0001$, $t(10) = 20.792$ shADSL-2 vs. shADSL-2 + *ADSL*, $P < 0.0001$, $t(10) = 24.815$; 5d, shCont vs. shADSL-1, $P < 0.0001$, $t(10) = 17.779$; shCont vs. shADSL-2, $P < 0.0001$, $t(10) = 17.833$; shADSL-1 vs. shADSL-1 + *ADSL*, $P < 0.0001$, $t(10) = 14.576$; shADSL-2 vs. shADSL-2 + *ADSL*, $P < 0.0001$, $t(10) = 9.860$. (**k**) *GMPS*: 3d, shCont vs. shGMPS-1, $P < 0.0001$, $t(10) = 24.485$; shCont vs. shGMPS-2, $P < 0.0001$, $t(10) = 24.741$; shGMPS-1 vs. shGMPS-1 + *GMPS*, $P < 0.0001$, $t(10) = 20.847$; shGMPS-2 vs shGMPS-2 + *GMPS*, $P < 0.0001$, $t(10) = 26.123$; 5d, shCont vs. shGMPS-1, $P < 0.0001$, $t(10) = 19.968$; shCont vs. shGMPS-2, $P < 0.0001$, $t(10) = 20.034$; shGMPS-1 vs. shGMPS-1 + *GMPS*, $P < 0.0001$, $t(10) = 13.139$; shGMPS-2 vs. shGMPS-2 + *GMPS*, $P < 0.0001$, $t(10) = 16.020$. (**l**) *PRPS1*: 3d, shCont vs. shPRPS1-1, $P < 0.0001$, $t(10) = 14.668$; shCont vs. shPRPS1-2, $P < 0.0001$, $t(10) = 13.888$; shPRPS1-1 vs. shPRPS1-1 + *PRPS1*, $P < 0.0001$, $t(10) = 25.521$; shPRPS1-2 vs. shPRPS1-2 + *PRPS1*, $P < 0.0001$, $t(10) = 32.771$; 5d, shCont vs. shPRPS1-1, $P < 0.0001$, $t(10) = 15.793$; shCont vs. shPRPS1-2, $P < 0.0001$, $t(10) = 15.749$; shPRPS1-1 vs shPRPS1-1 + *PRPS1*, $P < 0.0001$, $t(10) = 15.179$; shPRPS1-2 vs. shPRPS1-2 + *PRPS1*, $P < 0.0001$, $t(10) = 16.676$. (**m**-**r**) Attenuation of purine synthesis pathway genes decreases levels of precursor markers. The expression levels of three purine synthesis pathway genes (*ADSL*, *GMPS*, and *PRPS1*) were knocked down using shRNAs in (**m**-**o**) T387 and (**p**-**r**) T4121 BTICs. Two independent shRNAs were used for each gene, and shCont was used as a control. Quantitative RT-PCR assessment was performed for precursor markers (*SOX2*, *NES*, and *OLIG2*), and differentiation markers (*GFAP* and *MBPF*). All statistical analyses were performed using two-tailed unpaired Student's t-test; **, $P < 0.01$; n = 3 independent experiments per group. Data were presented as median ± s.e.m. (**m**) shADSL/T387: *SOX2*, shADSL-1, $P < 0.0001$, $t(4) = 14.673$; shADSL-2, $P < 0.0001$, $t(10) = 17.606$. *NES*, shADSL-1, $P = 0.0002$, $t(4) = 11.146$; shADSL-2, $P < 0.0001$, $t(4) = 16.397$. *OLIG2*, shADSL-1, $P < 0.0001$, $t(4) = 58.604$; shADSL-2, $P < 0.0001$, $t(4) = 79.446$. *GFAP*, shADSL-1, $P = 0.0006$, $t(4) = 8.312$; shADSL-2, $P = 0.0001$, $t(4) = 12.230$. *MBPF*, shADSL-1, $P < 0.0001$, $t(4) = 28.772$; shADSL-2, $P = 0.0001$, $t(4) = 12.936$. (**n**) shGMPS/T387: *SOX2*, shGMPS-1, p = 0.0017 $P < 0.0001$, $t(4) = 6.174$; shGMPS-2, $P = 0.0022$, $t(4) = 5.770$. *NES*, shGMPS-1, $P = 0.0006$, $t(4) = 8.178$; shGMPS-2, $P = 0.0004$, $t(4) = 9.273$. *OLIG2*, shGMPS-1, $P < 0.0001$, $t(4) = 21.918$; shGMPS-2, $P < 0.0001$, $t(4) = 20.266$. *GFAP*, shGMPS-1, $P = 0.0006$, $t(4) = 8.254$; shGMPS-2, $P = 0.0001$, $t(4) = 12.016$. *MBPF*, shGMPS-1, $P < 0.0001$, $t(4) = 19.169$; shGMPS-2, $P < 0.0001$, $t(4) = 17.426$. (**o**) shPRPS1/T387: *SOX2*, shPRPS1-1, $P < 0.0001$, $t(4) = 15.687$; shPRPS1-2, $P < 0.0001$, $t(4) = 14.160$. *NES*, shPRPS1-1, $P <$

0.0001, $t(4) = 13.845$; shPRPS1-2, $P < 0.0001$, $t(4) = 16.453$. *OLIG2*, shPRPS1-1, $P = 0.0008$, $t(4) = 7.737$; shPRPS1-2, $P = 0.0005$, $t(4) = 8.555$. *GFAP*, shPRPS1-1, $P < 0.0001$, $t(4) = 15.062$; shPRPS1-2, $P = 0.0010$, $t(4) = 7.229$. *MBPF*, shPRPS1-1, $P < 0.0001$, $t(4) = 18.115$; shPRPS1-2, $P = 0.0002$, $t(4) = 11.449$. (**p**) shADSL/T4121: *SOX2*, shADSL-1, $P < 0.0001$, $t(4) = 21.903$; shADSL-2, $P < 0.0001$, $t(4) = 21.559$. *NES*, shADSL-1, $P < 0.0001$, $t(4) = 13.181$; sh-2, $P = 0.0001$, $t(4) = 12.622$. *OLIG2*, shADSL-1, $P < 0.0001$, $t(4) = 35.077$; shADSL-2, $P < 0.0001$, $t(4) = 33.981$. *GFAP*, shADSL-1, $P = 0.0017$, $t(4) = 6.204$; shADSL-2, $P = 0.0067$, $t(4) = 4.227$. *MBPF*, shADSL-1, $P = 0.0005$, $t(4) = 8.531$; shADSL-2, $P = 0.0002$, $t(4) = 10.723$. (**q**) shGMPS/T4121: *SOX2*, shGMPS-1, $P < 0.0001$, $t(4) = 24.236$; shGMPS-2, $P < 0.0001$, $t(4) = 35.825$. *NES*, shGMPS-1, $P = 0.0003$, $t(4) = 9.719$; shGMPS-2, $P = 0.0001$, $t(4) = 12.040$. *OLIG2*, shGMPS-1, $P < 0.0001$, $t(4) = 15.920$; shGMPS-2, $P < 0.0001$, $t(4) = 17.743$. *GFAP*, shGMPS-1, $P = 0.0003$, $t(4) = 10.097$; shGMPS-2, $P = 0.0011$, $t(4) = 7.052$. *MBPF*, shGMPS-1, $P < 0.0001$, $t(4) = 14.167$; shGMPS-2, $P = 0.0006$, $t(4) = 8.057$. (**r**) shPRPS1/T4121: *SOX2*, shPRPS1-1, $P = 0.0003$, $t(4) = 9.883$; shPRPS1-2, $P = 0.0010$, $t(4) = 7.120$. *NES*, shPRPS1-1, $P < 0.0001$, $t(4) = 13.532$; shPRPS1-2, $P = 0.0008$, $t(4) = 7.601$. *OLIG2*, shPRPS1-1, $P = 0.0002$, $t(4) = 10.928$; shPRPS1-2, $P = 0.0003$, $t(4) = 10.153$. *GFAP*, shPRPS1-1, $P < 0.0001$, $t(4) = 20.580$; shPRPS1-2, $P = 0.0001$, $t(4) = 12.366$. *MBPF*, shPRPS1-1, $P = 0.0108$, $t(4) = 3.658$; shPRPS1-2, $P = 0.0024$, $t(4) = 5.659$.

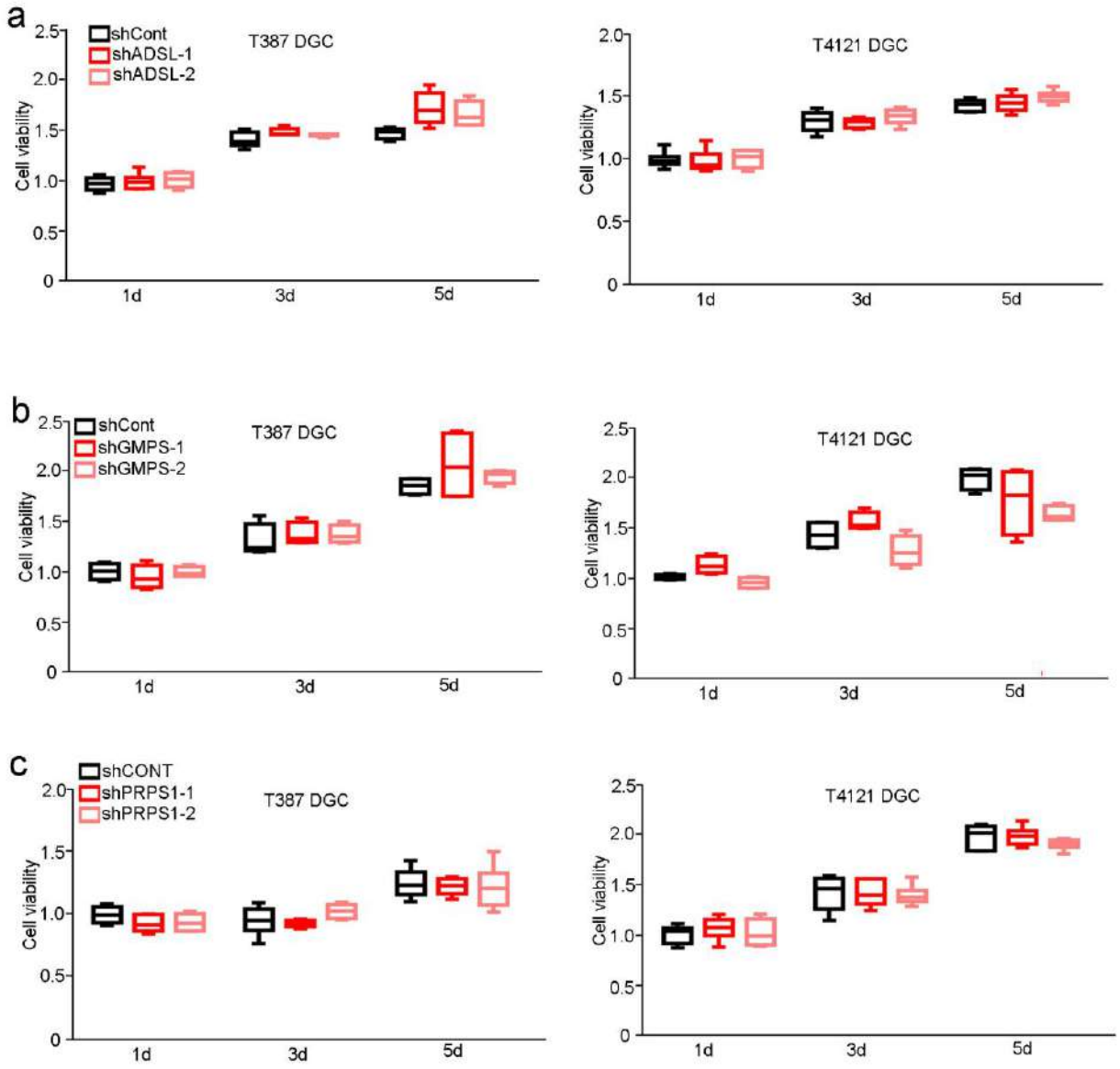

Supplementary Figure 10

Purine synthesis enzymes are dispensable in DGCs.

(**a**) Cell viability of T387 and T4121 DGCs expressing non-targeting control shRNA (shCont), shADSL-1, or shADSL-2. All statistical analyses were performed using two-tailed unpaired Student's t-test; n = 6 independent experiments per group. (T387: shADSL-1, 3d, P = 0.0898, $t(10)$ = 1.901; 5d, P = 0. 0.6953, $t(10)$ = 0.405. shADSL-2, 3d, P = 0. 0.2007, $t(10)$ = 1.381; 5d, P = 0.0.3285, $t(10)$ = 1.033. T4121: shADSL-1, 3d, P = 0. 0.7437, $t(10)$ = 0.336; 5d, P = 0.5498, $t(10)$ = 0.619. shADSL-2, 3d, P = 0.0.4010, $t(10)$ = 0.877; 5d, P = 0. 0.1005, $t(10)$ = 1.857.) (**b**) Cell viability of T387 and T4121 DGCs expressing shCont, shGMPS-1, or shGMPS-2. All statistical analyses were performed using two-tailed unpaired Student's t-test; n = 6 independent experiments per group. (T387: shGMPS-1, 3d, P = 0. 0.5411, $t(10)$ = 0.648; 5d, P = 0. 5498, $t(10)$ = 0.619. shGMPS-2, 3d, P = 0. 5308, $t(10)$ = 0.665; 5d, P = 0. 1243, $t(10)$ = 1.786. T4121: shGMPS-1, 3d, P = 0. 1611, $t(10)$ = 1.598; 5d, P = 0. 2542, $t(10)$ = 1.261. shGMPS-2, 3d, P = 0. 1765, $t(10)$ = 1.532; 5d, P = 0. 1334, $t(10)$ = 1.735.) (**c**) Cell viability of T387 and T4121 DGCs expressing shCont, shPRPS1-1, or shPRPS1-2. All statistical analyses were performed using two-tailed unpaired Student's t-test; n = 6 independent experiments per group. (T387: shPRPS1-1, 3d, P = 0. 6128, $t(10)$ = 0.509; 5d, P = 0. 6473 $t(10)$ = 0.433. shPRPS1-2, 3d, P = 0. 1689, $t(10)$ = 1.483; 5d, P = 0. 7176, $t(10)$ = 0.372. T4121: shPRPS1-1, 3d, P = 0. 9627, $t(10)$ = 0.048; 5d, P = 0. 9848, $t(10)$ = 0.019. shPRPS1-2, 3d, P = 0. 7391, $t(10)$ = 0.342; 5d, P = 0. 1960, $t(10)$ = 1.385.)

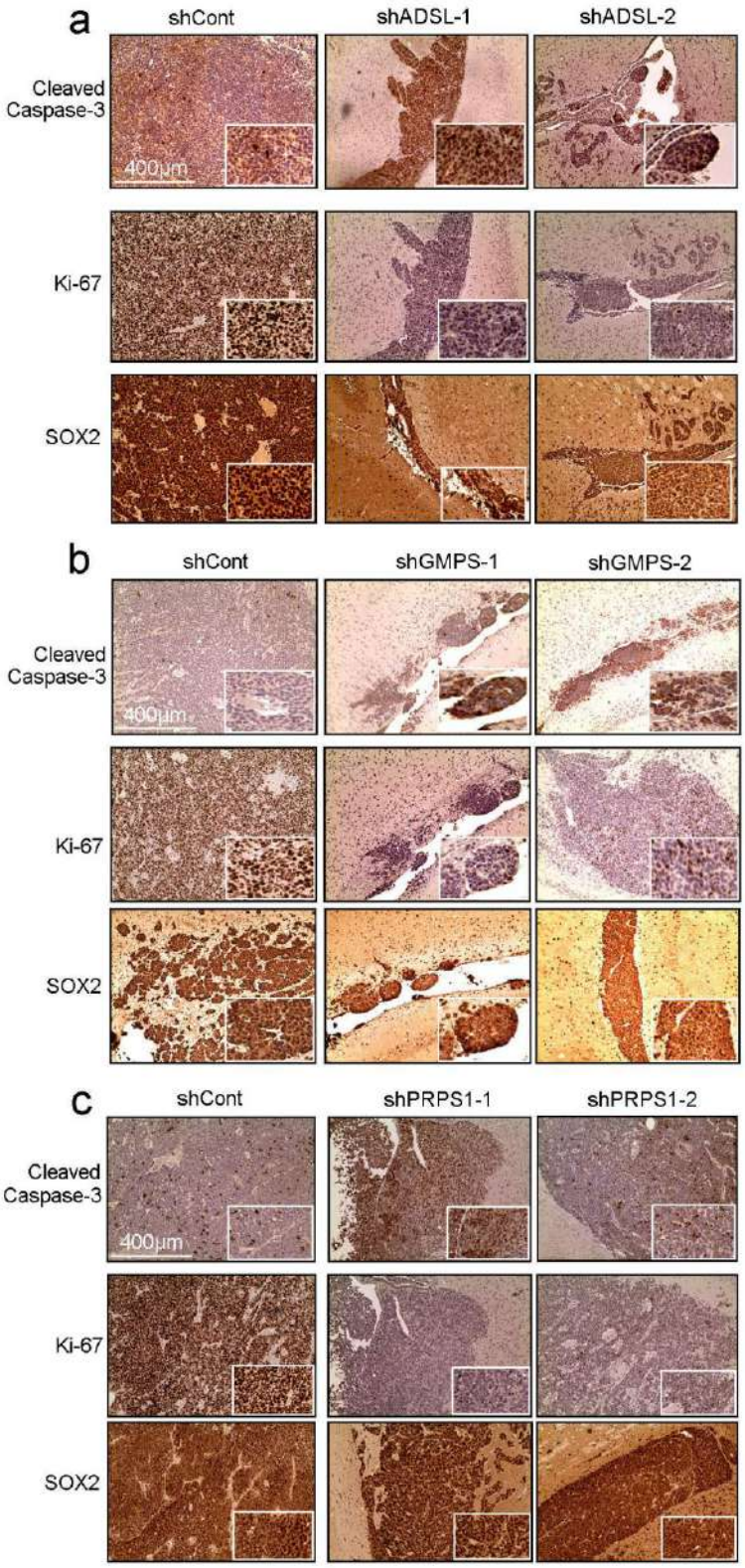

Supplementary Figure 11

***In vivo* impact of targeting purine synthesis enzymes on proliferation, apoptosis and stemness.**

(**a**) Representative images of immunohistochemical (IHC) staining of cross-sections of mouse brains harvested on day 18 after transplantation of T387 BTICs expressing shCont, shADSL-1, or shADSL-2. Ki-67, cleaved Caspase-3, and *SOX2* were employed as markers of proliferation, apoptosis, and stemness respectively. Each image was representative for at least 3 similar experiments. (**b**) Representative images of IHCstaining of cross-sections of mouse brains harvested on day 18 after transplantation of T387 BTICs expressing shCont, shGMPS-1, or shGMPS-2. Each image was representative for at least 3 similar experiments. (**c**) Representative images of IHC staining of cross-sections of mouse brains harvested on day 18 after transplantation of T387 BTICs expressing shCont, shPRPS1-1, or shPRPS1-2. Each image was representative for at least 3 similar experiments.

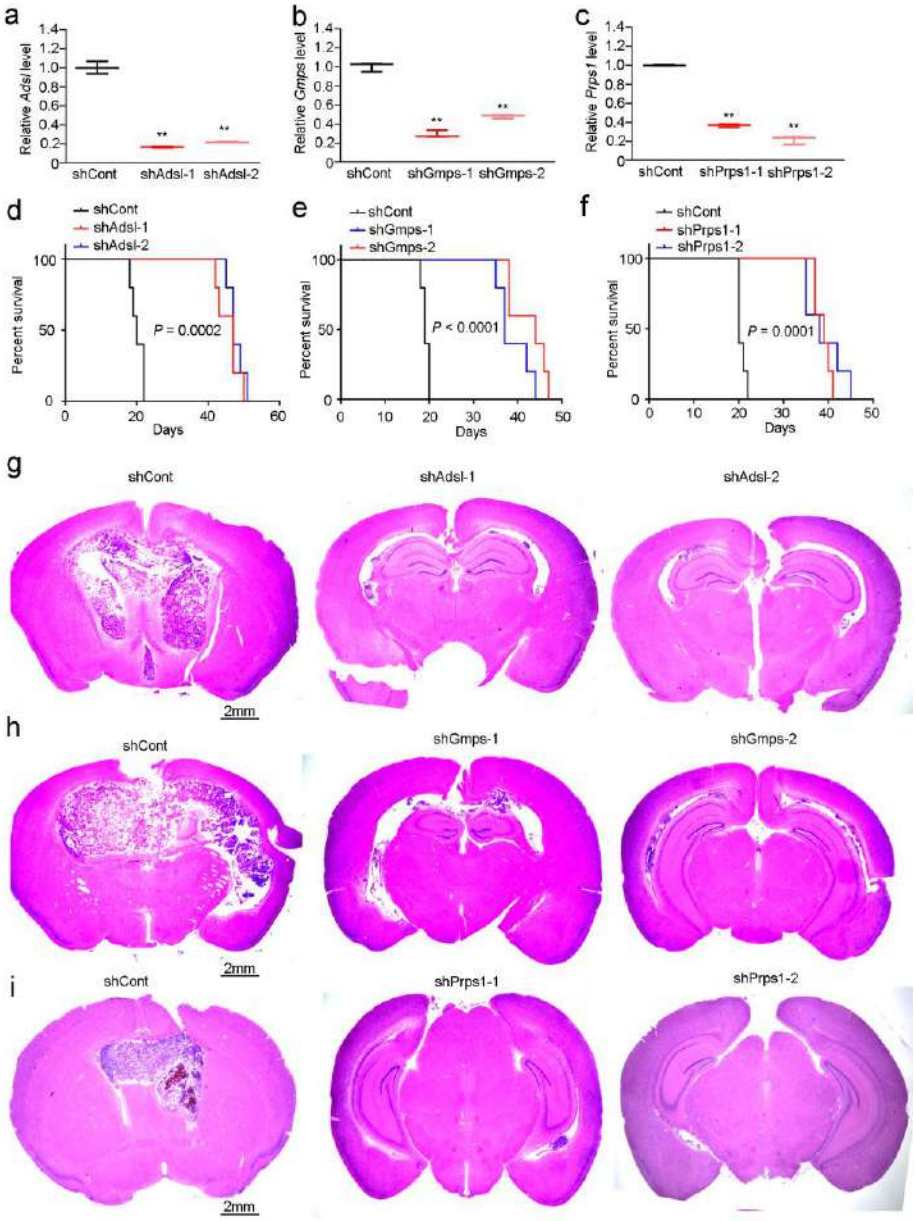

Supplementary Figure 12

Purine synthesis regulates *in vivo* BTIC tumorigenesis in an immunocompetent mouse model.

(**a**-**c**) Successful targeting of three purine synthetic genes: (a) *Adsl*, (b) *Gmps*, and *Prps1*, in the murine GL261 glioma line was confirmed by RT-PCR. All statistical analyses were performed using two-tailed unpaired Student's t-test; **, $P < 0.01$; n = 3 independent experiments per group. Data were presented as median ± s.e.m. (shAdsl-1, $P < 0.0001$, $t(4) = 22.059$; shAdsl-2, $P < 0.0001$, $t(4) = 20.764$. shGmps-1, $P < 0.0001$, $t(4) = 20.040$; shGmps-2, $P < 0.0001$, $t(4) = 17.503$. shPrps1-1, $P < 0.0001$, $t(4) = 61.767$; shPrps1-2, $P < 0.0001$, $t(4) = 30.503$.) (**d**-**f**) Kaplan-Meier survival curves of MHC-matched B6 immunocompetent mice bearing intracranial glioma 261 (GL261) BTICs, transduced with shCont, shAdsl, shGmps, or shPrps1 are displayed. For each target, two, non-overlapping shRNAs were used. n = 5 animals per group. Statistical analysis was performed using log-rank test. **, p < 0.01. (shAdsl: $P = 0.0002$; shGmps: $P < 0.0001$; shPrps1: $P = 0.0001$.) (**g**-**i**) Representative images of hematoxylin and eosin stained cross-sections of B6 mouse brains harvested on day 18 after transplantation of GL216 BTICs expressing shCont, shAdsl-1, shAdsl-2, shGmps-1, shGmps-2, shPrps1-1, or shPrps1-2 are shown. Scale bar, 2 mm. Each image was representative for at least 3 similar experiments.

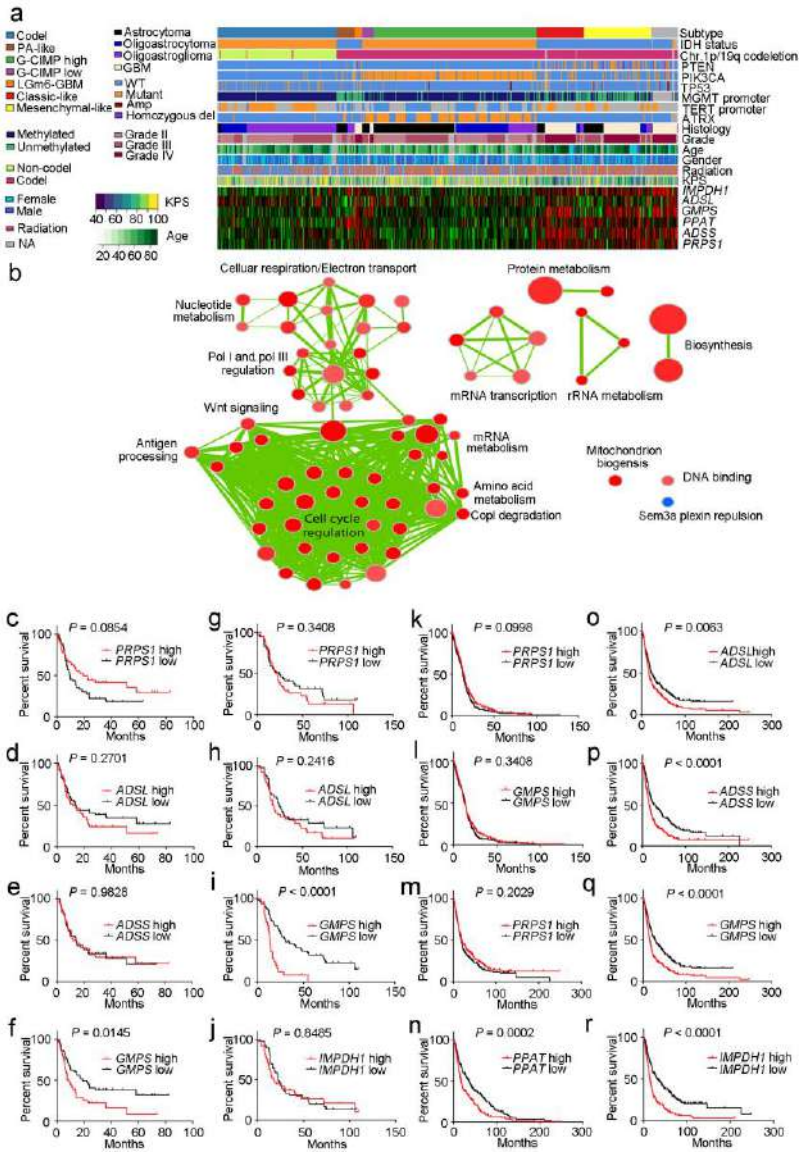

Supplementary Figure 13

Purine synthesis enzymes are expressed in non-G-CIMP gliomas.

(**a**) Investigation of purine pathway gene expression in the pan-glioma TCGA cohort demonstrates enrichment in high grade glioma. (**b**) Gene set enrichment analysis reveals significant positive correlation of the purine metabolic signature with regulation of cell cycle and transcriptional activity. (**c**-**f**) Survival analysis of the Freije high-grade glioma dataset for *PRPS1*, ADSL, ADSS, and GMPS. All statistical analyses were performed using log-rank test. (*PRPS1*^{low}, n = 44; *PRPS1*^{high}, n = 41; *P* = 0.0854. *ADSL*^{low}, n = 43; *ADSL*^{high}, n = 42; *P* = 0.2701. *ADSS*^{low}, n = 43; *ADSS*^{high}, n = 42; *P* = 0.9828. *GMPS*^{low}, n = 51; *GMPS*^{high}, n = 34; *P* = 0.0145.) (**g**-**j**) Survival analysis of the Phillips high-grade glioma dataset for *PRPS1*, ADSL, GMPS, and IMPDH. All statistical analyses were performed using log-rank test. (*PRPS1*^{low}, n = 39; *PRPS1*^{high}, n = 38; *P* = 0.3408. *ADSL*^{low}, n = 37; *ADSL*^{high}, n = 38; *P* = 0.2416. *GMPS*^{low}, n = 52; *GMPS*^{high}, n = 25; *P* < 0.0001. *IMPDH1*^{low}, n = 39; *IMPDH1*^{high}, n = 38; *P* = 0.8485.) (**k**,**l**) Survival analysis of the TCGA glioblastoma for *PRPS1* and GMPS. All statistical analyses were performed using log-rank test. (*PRPS1*^{low}, n = 244; *PRPS1*^{high}, n = 237; *P* = 0.098. *GMPS*^{low}, n = 230; *GMPS*^{high}, n = 251; *P* = 0.3408.) (**m**-**r**) Survival analysis of the REMBRANDT dataset for 6 enzymes in the purine synthesis pathway. All statistical analyses were performed using log-rank test. (*PRPS1*^{low}, n = 254; *PRPS1*^{high}, n = 255; *P* = 0.2029. *PPAT*^{low}, n = 254; *PPAT*^{high}, n = 255; *P* = 0.0002. *ADSL*^{low}, n = 254; *ADSL*^{high}, n = 255; *P* = 0.0063. *ADSS*^{low}, n = 254; *ADSS*^{high}, n = 255; *P* < 0.0001. *GMPS*^{low}, n = 254; *GMPS*^{high}, n = 255; *P* < 0.0001. *IMPDH1*^{low}, n = 254; *IMPDH1*^{high}, n = 255; *P* < 0.0001.)

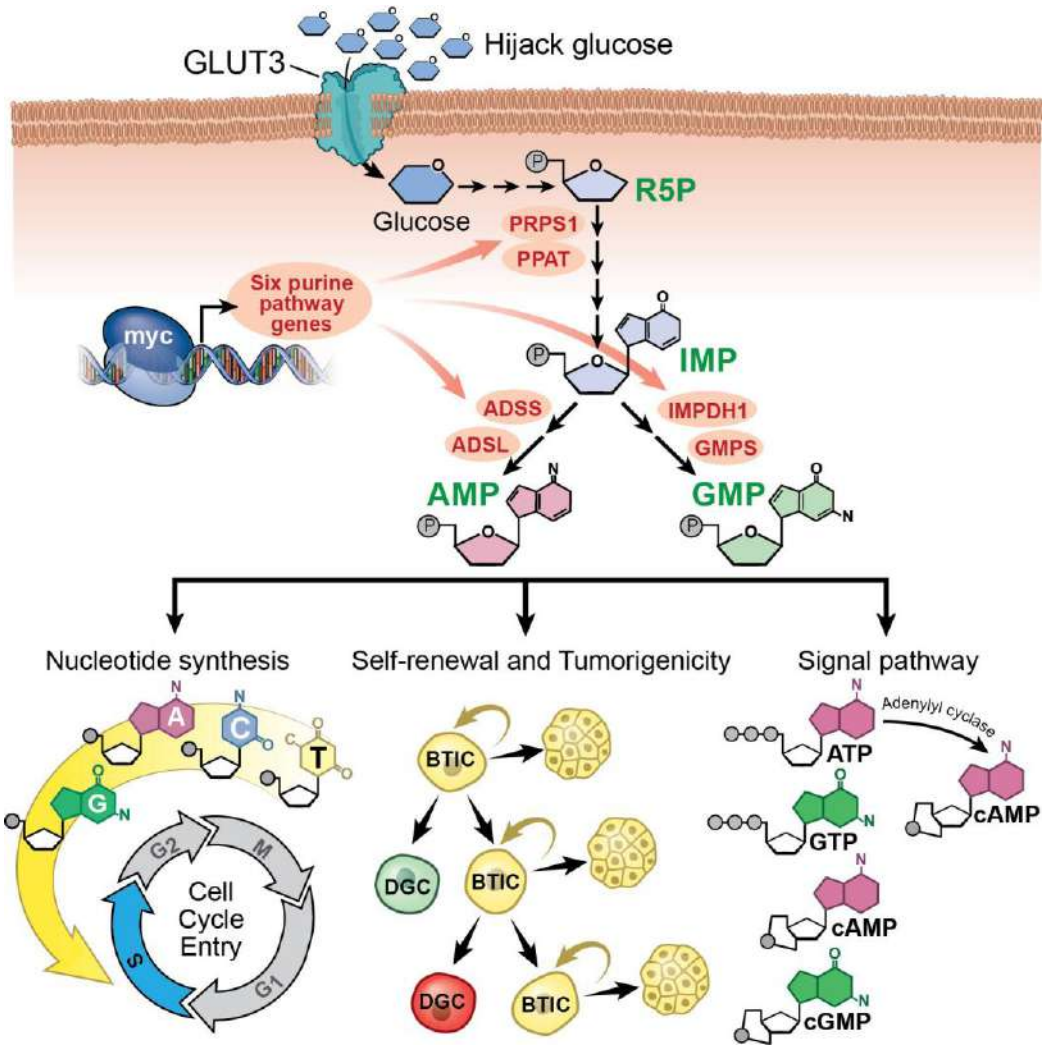

Supplementary Figure 14

Proposed model of purine biosynthesis in BTICs.

BTICs upregulate GLUT3 to hijack the neuronal survival mechanism to compete for glucose in a dynamic microenvironment. The increased carbon influx is channeled to the synthesis of purine nucleotides, mediated by the transcriptional factor MYC. Elevated levels of purine nucleotides promote BTIC maintenance through numerous mechanisms, including DNA synthesis, self-renewal and tumorigenecity, and signaling pathways.

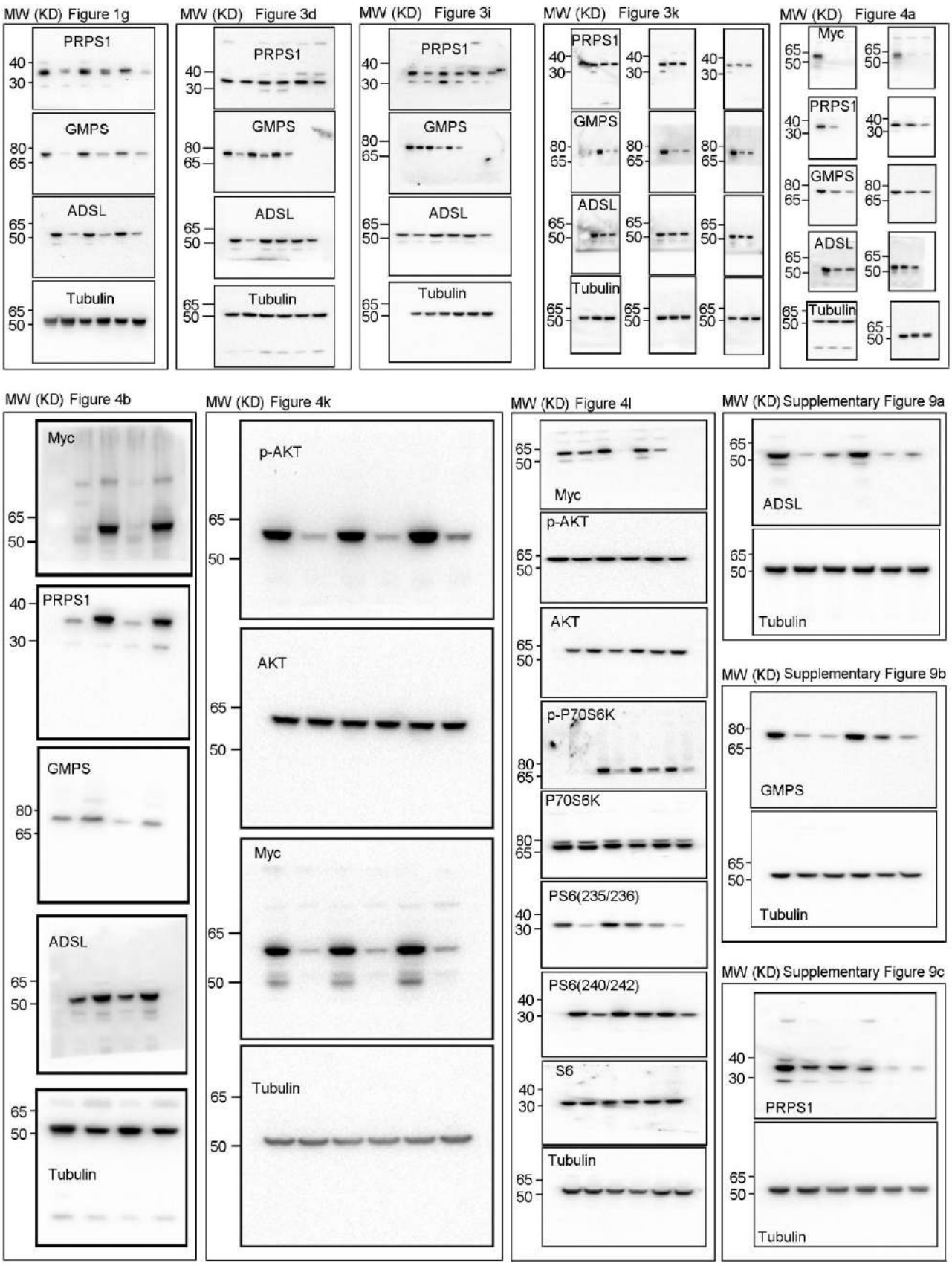

Nature Neuroscience: doi:10.1038/nn.4537

Supplementary Figure 15

Full-length Western blots.

Full-length Western blots for cropped images in Fig. 1g, 3d, 3i, 3k, 4a, 4b, 4k, 4l, and Supplementary Fig. 9a-c.

Purine Synthesis Promotes Maintenance of Brain Tumor Initiating Cells in Glioma

Supplementary Table 1. Gene set enrichment analysis for enhancers of metabolic signature genes comparing BTICs vs. DGCs from 3 primary glioblastoma specimens (MGG4, MGG6, and MGG8).

Pathway	***P* value**
Cholesterol	0.00262
Nucleotide	0.00459
Proton Transport	0.01647
Glycan Anchor	0.02254
Glycan	0.02307
Creatine	0.02599
Glycine	0.03504
Complex III	0.04538
Small Molecule Transport	0.06037
Signaling	0.06327
BCAAs	0.06883
Pentose Phosphate	0.06883
Redox	0.06981
Sugar	0.10475
Complex II	0.16470
Multipurpose	0.18593
Purine	0.24510
Aminosugar	0.25207
Glycolysis	0.25705
Histidine	0.27018
Methionine	0.27018
Sphingosine	0.27018

Urea	0.27018
Complex IV	0.28517
Ion Transport	0.29463
Krebs	0.30169
Mevalonate	0.30230
ABC Transporter	0.32982
Tyrosine	0.33300
Glycan Degradation	0.342004
Folate	0.39042
Amino Acid	0.41406
Carbohydrate Storage	0.44289
Neurotransmitter	0.51327
Fatty Acid	0.51870
NAD	0.53469
Complex I	0.54381
Detox	0.60674
Sulfate	0.61137
Sphingolipid	0.64484
Heparin Sulfate	0.66048
Pyrimidine	0.68972
Inositol Phosphate	0.72148
Glutathione	0.78359
Hormone	0.78359
Membrane Lipid	0.87147
Anaerobic Glycolysis	1
ATPase	1
B12	1
BH4	1
Bile Acid	1

CoA	1
Cofactor	1
Glutamate	1
Glycan Sulfate	1
Glyoxylate	1
Ketone Bodies	1
Lysine	1
Nucleotide Sugar	1
Pigment	1
Polyamine	1
Porphyrin	1
Proline	1
Propanoate	1
Reactive Oxygen	1
Serine	1
Steroid	1
Tryptophan	1
Ubiquinone	1
Vitamin A	1
Vitamin B6	1
Xylulose	1